A Direct Demonstration of Closed-State Inactivation of K^+ Channels at Low pH

Thomas W. Claydon,[1] Moni Vaid,[2] Saman Rezazadeh,[2] Daniel C.H. Kwan,[2] Steven J. Kehl,[2] and David Fedida[1,2]

[1]Department of Anesthesiology, Pharmacology, and Therapeutics and [2]Department of Cellular and Physiological Sciences, University of British Columbia, Vancouver, V6T 1Z3 Canada

Lowering external pH reduces peak current and enhances current decay in Kv and *Shaker-IR* channels. Using voltage-clamp fluorimetry we directly determined the fate of *Shaker-IR* channels at low pH by measuring fluorescence emission from tetramethylrhodamine-5-maleimide attached to substituted cysteine residues in the voltage sensor domain (M356C to R362C) or S5-P linker (S424C). One aspect of the distal S3-S4 linker α-helix (A359C and R362C) reported a pH-induced acceleration of the slow phase of fluorescence quenching that represents P/C-type inactivation, but neither site reported a change in the total charge movement at low pH. *Shaker* S424C fluorescence demonstrated slow unquenching that also reflects channel inactivation and this too was accelerated at low pH. In addition, however, acidic pH caused a reversible loss of the fluorescence signal ($pKa = 5.1$) that paralleled the reduction of peak current amplitude ($pKa = 5.2$). Protons decreased single channel open probability, suggesting that the loss of fluorescence at low pH reflects a decreased channel availability that is responsible for the reduced macroscopic conductance. Inhibition of inactivation in *Shaker* S424C (by raising external K^+ or the mutation T449V) prevented fluorescence loss at low pH, and the fluorescence report from closed *Shaker* ILT S424C channels implied that protons stabilized a W434F-like inactivated state. Furthermore, acidic pH changed the fluorescence amplitude ($pKa = 5.9$) in channels held continuously at −80 mV. This suggests that low pH stabilizes closed-inactivated states. Thus, fluorescence experiments suggest the major mechanism of pH-induced peak current reduction is inactivation of channels from closed states from which they can activate, but not open; this occurs in addition to acceleration of P/C-type inactivation from the open state.

INTRODUCTION

The kinetic properties of many voltage gated potassium (Kv) channels are affected by external pH. Low extracellular pH reduces the peak current in *Shaker* channels as well as in Kv1.3, Kv1.4, and Kv1.5 from the related Kv1 family of mammalian channels (Deutsch and Lee, 1989; Lopez-Barneo et al., 1993; Perez-Cornejo, 1999; Steidl and Yool, 1999; Claydon et al., 2000; Jäger and Grissmer, 2001; Kehl et al., 2002; Starkus et al., 2003; Somodi et al., 2004) in a manner that is independent of the depolarizing shift of the voltage dependence of channel opening that is caused by a proton-induced charge screening effect (Deutsch and Lee, 1989; Kehl et al., 2002; Trapani and Korn, 2003). In pH-sensitive mammalian Kv1 channels, a histidine residue in the outer pore is responsible for the inhibition of current and consistent with this, the pK_a (with physiological external K^+ concentrations) is pH 6.1–6.2 (Steidl and Yool, 1999; Claydon et al., 2000; Kehl et al., 2002). In the case of the *Shaker* channel, which does not possess a histidine residue within the outer pore, the pK_a is pH 4.7–5.0 suggesting that the pH sensor may be an aspartate or glutamate residue (Perez-Cornejo, 1999; Starkus et al., 2003).

In the absence of N-type inactivation, acidic pH not only reduces peak current amplitude, but also enhances the decay of current in *Shaker*, Kv1.4, and Kv1.5 channels during the depolarizing pulse (Perez-Cornejo, 1999; Claydon et al., 2002; Starkus et al., 2003; Zhang et al., 2003). It has been suggested that the decrease in peak current observed with extracellular acidification occurs as a direct consequence of the pH-induced enhancement of open-state inactivation, which results in an accumulation of channels in the P/C-type inactivated state (Steidl and Yool, 1999; Starkus et al., 2003; Zhang et al., 2003). In support of this, the acceleration of current decay and the decrease of peak current amplitude at low pH is abolished in *Shaker*, Kv1.4, and Kv1.5 mutant channels in which inactivation is compromised by mutation of the outer pore residue equivalent to T449 in *Shaker* (K532 and R487 in Kv1.4 and Kv1.5, respectively), to a valine or tyrosine residue (Claydon et al., 2002; Starkus et al., 2003; Zhang et al., 2003; Kurata and Fedida, 2006).

However, an additional mechanism to explain the decreased peak Kv channel current at low pH has also

Correspondence to David Fedida: fedida@interchange.ubc.ca

Abbreviations used in this paper: PMT, photomultiplier tube; TMRM, tetramethylrhodamine-5-maleimide.

J. Gen. Physiol. © The Rockefeller University Press $15.00
Volume 129 Number 5 May 2007 437–455
http://www.jgp.org/cgi/doi/10.1085/jgp.200709774

been proposed from our previous work. During extracellular acidification (to pH 5.9), Kv1.5 current inhibition did not demonstrate use dependence as would be expected if the current was being reduced by an accumulation of open-state inactivation (Kehl et al., 2002). In addition, a 2-min rest interval with pH 5.9 bath solution, which would allow enough time for recovery from pH-induced open-state inactivation, did not relieve the current inhibition, which suggests that inactivated channels cannot recover easily at low pH. This idea of stabilization of closed-state inactivated channels at low pH is supported by a recent study investigating the effect of acidic pH on single channel Kv1.5 current. Acidic pH did not alter the Kv1.5 single channel conductance, but increased the number of null sweeps and induced gating behavior in which the channel switched between available and unavailable modes (Kwan et al., 2006). This suggests that extracellular acidification reduces channel availability. Since low pH apparently also accelerated open-state inactivation, as the mean burst duration was decreased and the interburst interval was increased, these data suggest that extracellular acidification enhances both open- and closed-state inactivation, and that the two processes can coexist in Kv channels.

Voltage-clamp fluorimetry allows real-time observation of the conformational changes associated with channel gating, including those that do not result in ionic current flow (Mannuzzu et al., 1996; Cha and Bezanilla, 1997). Changes in the emission observed from a fluorophore attached at specific residues are due to changes of its microenvironment as channels activate and inactivate (Cha and Bezanilla, 1997; Loots and Isacoff, 1998; Bezanilla, 2002). Here, we have used this technique to investigate the fate of channels at low pH by directly monitoring the effect of acidification on the channel rearrangements associated with P-type, C-type, and closed-state inactivation of *Shaker* channels. We show that low extracellular pH not only enhances P-type inactivation of channels, but also their progression to the C-type inactivated state, and in addition that protons stabilize an unavailable state in which channels are inactivated at rest. We demonstrate that stabilization of closed-inactivated states at low pH is largely responsible for the decrease in peak current amplitude, while stabilization of open-inactivated states is responsible for the enhanced current decay. In parallel, we have obtained single channel and gating current data that are in accord with this hypothesis. These data provide a direct demonstration that protons alter both open- and closed-state inactivation of Kv channels.

MATERIALS AND METHODS

Solutions

For *Xenopus* oocytes, Barth's medium contained (in mM) 88 NaCl, 1 KCl, 2.4 $NaHCO_3$, 0.82 $MgSO_4$, 0.33 $Ca(NO_3)_2$, 0.41 $CaCl_2$, 20 HEPES, titrated to pH 7.5 using NaOH. ND96 bath solution contained (in mM) 96 NaCl, 3 KCl, 1 $MgCl_2$, 0.3 $CaCl_2$, titrated to pH 7.5, 6.0, 5.0, or 4.0 using NaOH or HCl. HEPES (5 mM) was used as the buffer for pH 7.5 and pH 6.0 solutions, while 5 mM MES was used to buffer pH 5.0 and pH 4.0 solutions. Tetramethylrhodamine-5-maleimide (TMRM; Invitrogen) labeling of oocytes was performed in a depolarizing solution consisting of (in mM) 99 KCl, 1 $MgCl_2$, 2 $CaCl_2$, and 5 HEPES, titrated to pH 7.5 using KOH and which contained 50 μM TMRM. To record *Shaker* channel gating currents from *tsa201* cells, the pipette contained (in mM) 140 NMG, 1 $MgCl_2$, 10 EGTA, 10 HEPES, titrated to pH 7.5 using HCl, and the bath solution contained (in mM) 140 NMG, 1 $MgCl_2$, 10 HEPES, titrated to pH 7.5 or pH 4.0 using HCl. To record *Shaker* single channel activity from *ltk*− cells, the pipette contained (in mM) 130 KCl, 10 EGTA, 1.38 $MgCl_2$ (free concentration, 1 mM), 4.75 $CaCl_2$ (free concentration, 50 nM), 10 HEPES, titrated to pH 7.4 using KOH, and the bath solution contained (in mM) 3.5 KCl, 140 NaCl, 2 $CaCl_2$, 1 $MgCl_2$, 10 HEPES or MES, titrated to pH 7.4 or pH 4.0 using NaOH or HCl. Unless stated, all chemicals were purchased from Sigma-Aldrich.

Molecular Biology and RNA Preparation

The N-terminal deletion mutant *Shaker* Δ6–46 (*Shaker-IR*) that is fast inactivation removed (Hoshi et al., 1991) was expressed in *Xenopus* oocytes using a modified pBluescript SKII expression vector (pEXO) (a gift from A. Sivaprasadarao, University of Leeds, Leeds, UK) and in *ltk*− and *tsa201* mammalian cells using the GW1 vector (a gift from G. Panyi, University of Debrecen, Debrecen, Hungary). For oocyte fluorescence experiments, cysteine residues were introduced at specific sites (M356-R362) in the S3–S4 linker and S4 voltage sensor, and S424 in the S5-P turret for TMRM labeling and the only externally accessible cysteine residue, found in the S1–S2 linker, was replaced with a valine residue (C245V) to prevent nonspecific dye labeling. For clarity, we use the terms *Shaker* A359C and *Shaker* S424C to describe the *Shaker* Δ6–46 C245V A359C and *Shaker* Δ6–46 C245V S424C mutant channels, respectively. The T449V mutation in *Shaker* was used to inhibit slow inactivation (Lopez-Barneo et al., 1993) and the W434F mutation was used to permanently P-type inactivate channels (Perozo et al., 1993; Yang et al., 1997). The ILT mutant channel was a gift from E. Isacoff (University of California, Berkeley, CA) and was used to isolate the independent voltage sensor transitions from the concerted opening transition (Smith-Maxwell et al., 1998a,b). Point mutations were generated using the Stratagene Quikchange kit (Stratagene). All primers were synthesized by Sigma Genosys. All constructs were sequenced at the University of British Columbia core facility. cDNA was linearized using BstEII or HindIII (for ILT channels) and cRNA was synthesized using the mMessage mMachine T7 Ultra cRNA transcription kit (Ambion).

Oocyte Preparation and Injection

Xenopus laevis oocytes were prepared and isolated as described previously (Claydon et al., 2000). In brief, gravid frogs were terminally anesthetized, and stage V–VI oocytes were isolated and defolliculated using a combination of collagenase treatment (1 h in 1 mg/ml collagenase type 1; Sigma-Aldrich) and manual defolliculation. Oocytes were injected with 50 nl (5–10 ng) cRNA using a Drummond digital microdispenser (Fisher Scientific) and then incubated in Barth's medium at 19°C. Currents were recorded 1–7 d after injection.

Voltage-Clamp Fluorimetry

Voltage-clamp fluorimetry was performed as described previously (Claydon et al., 2006). In brief, introduced cysteine residues were labeled with 50 μM TMRM in oocyte depolarizing solution. Fluorimetry was performed using a Nikon TE300 inverted microscope with epifluorescence attachment and a 9124b Electron Tubes

TABLE I

Time Constants of Ionic Inactivation and Fluorescence Decay

	−TMRM		+TMRM	
	τ (s) at pH 7.5	τ (s) at pH 4.0	τ (s) at pH 7.5	τ (s) at pH 4.0
Ionic current				
Wild-type	5.7 ± 0.7 (8)	0.61 ± 0.11 (8)	3.9 ± 0.5 (4)	0.49 ± 0.07 (3)
A359C	5.6 ± 0.5 (10)	0.81 ± 0.18 (9)	*2.7 ± 0.2 (14)	0.58 ± 0.08 (11)
S424C	*1.5 ± 0.2 (7)	0.25 ± 0.05 (7)	*2.0 ± 0.3 (9)	0.26 ± 0.03 (5) (pH 5.0)
Fluorescence decay				
A359C	–	–	2.4 ± 0.3 (14)	1.2 ± 0.1 (14)
S424C	–	–	τ_1 2.6 ± 0.8 (9)	τ_1 0.33 ± 0.08 (5) (pH 5.0)
			τ_2 43.7 ± 22.2 (9)	τ_2 61.2 ± 52.4 (5) (pH 5.0)

Introduction of a cysteine residue at A359 had no effect on the inactivation of ionic current, but TMRM labeling of A359C accelerated inactivation to a certain degree. Introduction of a cysteine residue at S424C accelerated the inactivation of ionic current, but TMRM labeling had no additional effect. During prolonged depolarizing pulses (42 s), S424C fluorescence decay was best described by a biexponential function, which represents P- and C-type inactivation processes. Numbers in parentheses represent the number of oocytes measured. * represents inactivation time constants that were significantly different ($P < 0.05$) from the time constant of wild-type channel ionic current inactivation at pH 7.5 in the absence of TMRM (−TMRM, pH 7.5).

photomultiplier tube (PMT) module (Cairn Research). TMRM was excited by light filtered with a 525-nm band pass excitation filter and the fluorescence emission was collected using a 20× objective and filtered through a 565-nm long pass emission filter before being passed to the PMT recording module. Voltage signals from the PMT were then digitized using an Axon Digidata 1322 A/D converter and passed to a computer running pClamp9 software (Axon Instruments) to record the fluorescence emission intensity. To minimize fluorophore bleaching, a computer-controlled shutter (Uniblitz; Vincent Associates) was opened shortly before voltage-clamp pulses were applied. Fluorescence signals were filtered at 1 kHz with a sampling frequency of 20 kHz (when the pulse duration was 100 ms), 10 kHz (when the pulse duration was 7 s), or 2 kHz (when the pulse duration was 42 s). Traces were not averaged, except for those recorded during 100-ms pulses, which represent the average of five sweeps. To account for the bleaching of the fluorescence signal during 7- or 42-s pulses, fluorescence recorded for 7 or 42 s at the holding potential of −80 mV was subtracted. Simultaneous voltage clamp of the oocyte and acquisition of the current and voltage signals was achieved using the two-microelectrode voltage-clamp technique with a Warner Instruments OC-725C amplifier, Axon Digidata 1322, and pClamp9 software. Microelectrodes were filled with 3 M KCl and had a resistance of 0.2–0.5 MΩ.

Unlabeled wild-type *Shaker* channels inactivate with a time constant of 5.7 ± 0.7 s, and unlabeled *Shaker* A359C and S424C mutant channels inactivate with time constants of 5.6 ± 0.5 and 1.5 ± 0.2 s, respectively. This suggests that the introduction of a cysteine residue at S424, but not A359, speeds inactivation significantly. Despite this change, we believe that both the inactivation process and the nature of the fluorescence changes are qualitatively similar in their fast and slow components. First, we have shown that low pH accelerates inactivation of wild-type, A359C, and S424C channels similarly (9.4-, 6.9-, and 5.7-fold, respectively; the time constants of inactivation were reduced to 0.61 ± 0.11 s, 0.81 ± 0.18 s, and 0.25 ± 0.05 s, respectively). As well, other interventions that are known to modify inactivation such as raised external K^+, the mutation C462A in S6, and also low pH (Loots and Isacoff, 1998) result in consistent changes in ionic current and fluorescence measurements. This suggests that the underlying processes being examined are not seriously perturbed in these two cysteine-substituted channels. TMRM-labeled *Shaker* A359C and S424C channels inactivate with time constants of 2.7 ± 0.2 and 2.0 ± 0.3 s, respectively. Loots and Isacoff (1998) reported an inactivation time constant for TMRM-labeled S424C of 2.5 s, but a value for inactivation of ionic current in A359C mutant channels has not been reported previously. Our data suggest that TMRM labeling of A359C, but not S424C, speeds inactivation twofold (Table I). However, as suggested above, inactivation in TMRM-labeled A359C channels remains modifiable by low pH (the time constant of inactivation is reduced 4.6-fold to 0.58 ± 0.08 s at pH 4.0) and the overall effect is relatively unchanged. This also holds true for the pH sensitivity of TMRM-labeled S424C channels, which was somewhat greater than in unlabeled channels.

Single Channel and Gating Current Recordings

Single channel and gating currents were recorded using an Axopatch 200A amplifier (Axon Instruments) with computer-driven protocols (pClamp9 software and Digidata 1200B interface; Axon Instruments) or with an EPC-7 patch-clamp amplifier and Pulse + PulseFit software (HEKA Electronik). Single channel recordings were obtained from outside-out patches excised from *ltk*− cells expressing *Shaker* Δ6–46 channels. Currents were recorded during 500-ms voltage-clamp pulses to +100 mV from a holding potential of −80 mV (the pulse interval was 15 s). Data were sampled at 10 kHz and filtered at 1 kHz. Thin-walled borosilicate microelectrodes were coated with Sylgard (Dow Corning) and typically had a resistance of 8–12 MΩ. Gating current records were obtained in the whole-cell patch clamp configuration from *tsa201* cells expressing *Shaker* Δ6–46 channels. Currents were recorded during 20-ms voltage-clamp pulses from −80 to +80 mV in 10-mV increments from a holding potential of −80 mV. Leak subtraction was performed using a −P/4 protocol from a holding potential of −80 mV. Data were sampled at 100 kHz and filtered at 10 kHz. Microelectrodes had a resistance of 1.5–2.0 MΩ. Experiments were performed at 20–25°C.

Data Analysis

G-V curves were derived using the normalized chord conductance, which was calculated by dividing the maximum current during a depolarizing step by the driving force derived from the K^+ equilibrium potential (the internal K^+ concentration was assumed to be 99 mM). *G-V*, *F-V*, and *Q-V* curves were fitted with a single Boltzmann function:

$$y = 1/(1 + \exp((V_{1/2} - V)/k)), \quad (1)$$

where y is the conductance normalized with respect to the maximal conductance, $V_{1/2}$ is the half-activation potential, V is the test voltage, and k is the slope factor. Data throughout the text and figures are shown as mean ± SEM.

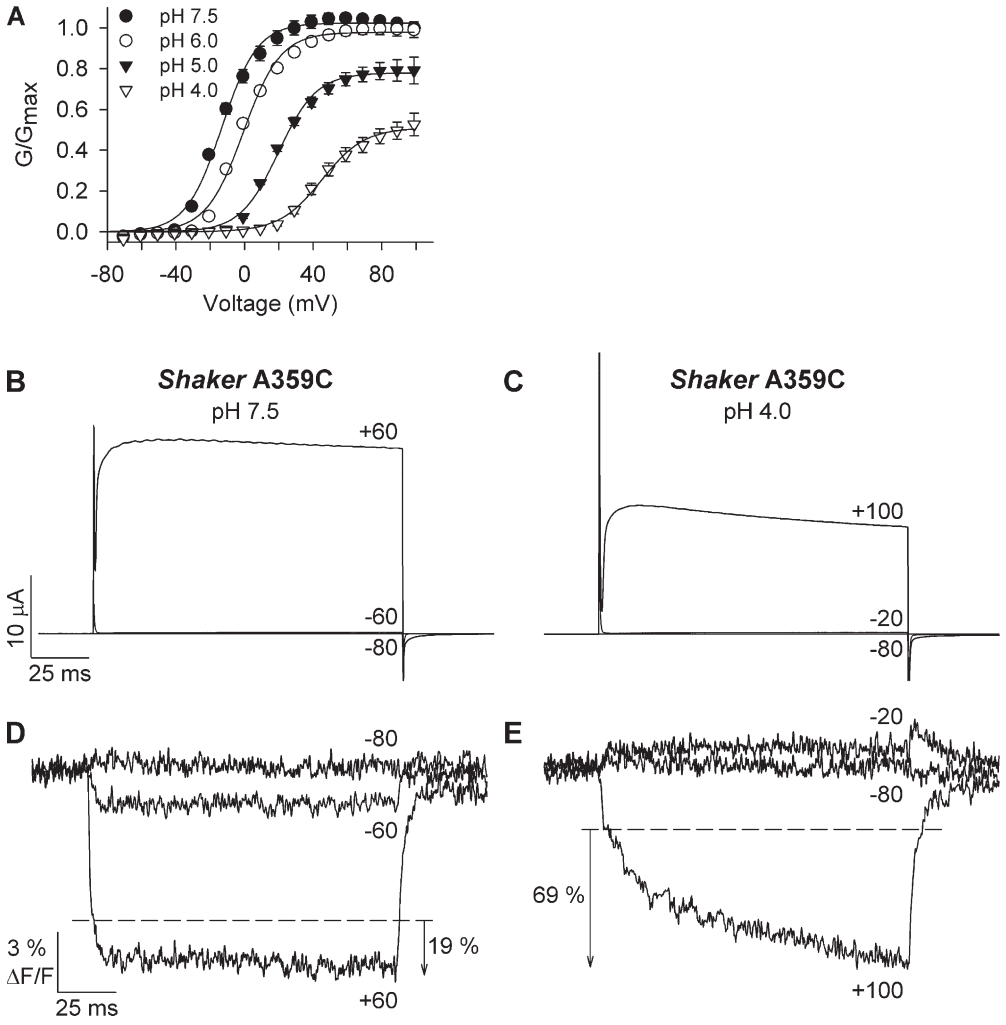

Figure 1. Low pH reduces the conductance of *Shaker* channels. (A) *G-V* relations of *Shaker* Δ6–46 channels recorded with the indicated external pH ($n = 3$). Conductance was calculated from currents recorded during 100-ms voltage pulses applied from −80 to +100 mV at 10-s intervals in 10-mV increments (holding potential −80 mV). (B–E) Typical ionic currents (B and C) and fluorescence signals (D and E) recorded from *Shaker* A359C channels in response to 100-ms voltage pulses applied from −80 to +100 mV at 10-s intervals (holding potential −80 mV) at pH 7.5 and pH 4.0. Although pulses were applied in 10-mV increments, only selected pulses are shown for clarity. Current and fluorescence traces at pH 4.0 (C and E) are shown at more depolarized potentials than in B and D to account for the charge screening effect of protons. Contributions of the fast and slow phases to the overall fluorescence signal were measured from biexponential fits of the fluorescence traces at +60 mV for pH 7.5 and at +100 mV for pH 4.0. Arrows and percentages in D and E show the contribution of the slow phase at pH 7.5 and pH 4.0. The mean slow phase contribution was 14 ± 2% at pH 7.5 and 71 ± 3% at pH 4.0 ($n = 8$).

RESULTS

Acidic pH Reduces the Conductance of *Shaker* Δ6–46 Channels

Shaker Δ6–46 currents are inhibited by extracellular protons ($pK_a \sim 4.7$–5.0) and this has been attributed to enhanced P/C-type open-channel inactivation at low pH (Perez-Cornejo, 1999; Starkus et al., 2003) that accumulates during repetitive stimulation (Starkus et al., 2003). However, we found that acidic extracellular pH reduced current amplitude even when the acceleration of inactivation during the depolarization was minimal, suggesting that protons also reduce the macroscopic conductance. This is shown in Fig. 1 A in the comparison of conductance–voltage relations at different external pH, which were constructed from currents recorded in response to short voltage-clamp pulses (100 ms) and with long interpulse intervals (10 s) to avoid cumulative inactivation. In addition to a rightward shift of the voltage dependence of channel opening that is attributed to a surface charge-screening effect (Deutsch et al., 1989; Hille, 2001; Kehl et al., 2002; Trapani and Korn, 2003), the maximal conductance was reduced at pH 5.0 by 21 ± 7% and at pH 4.0 by 47 ± 5% ($n = 3$).

Acidic pH Alters the Fluorescence Report from *Shaker* A359C Channels

Using voltage-clamp fluorimetry, it is possible to track the protein conformational rearrangements that are associated with ion channel gating (Mannuzzu et al., 1996; Cha and Bezanilla, 1997). Of particular importance to this study, this technique allows observation of electrically silent rearrangements that do not result in channel opening. We therefore used voltage-clamp fluorimetry to understand the fate of *Shaker* channels at low pH.

Data in Fig. 1 (B–E) show ionic current traces and fluorescence signals recorded from *Shaker* A359C channels with an extracellular pH of either 7.5 or 4.0. TMRM

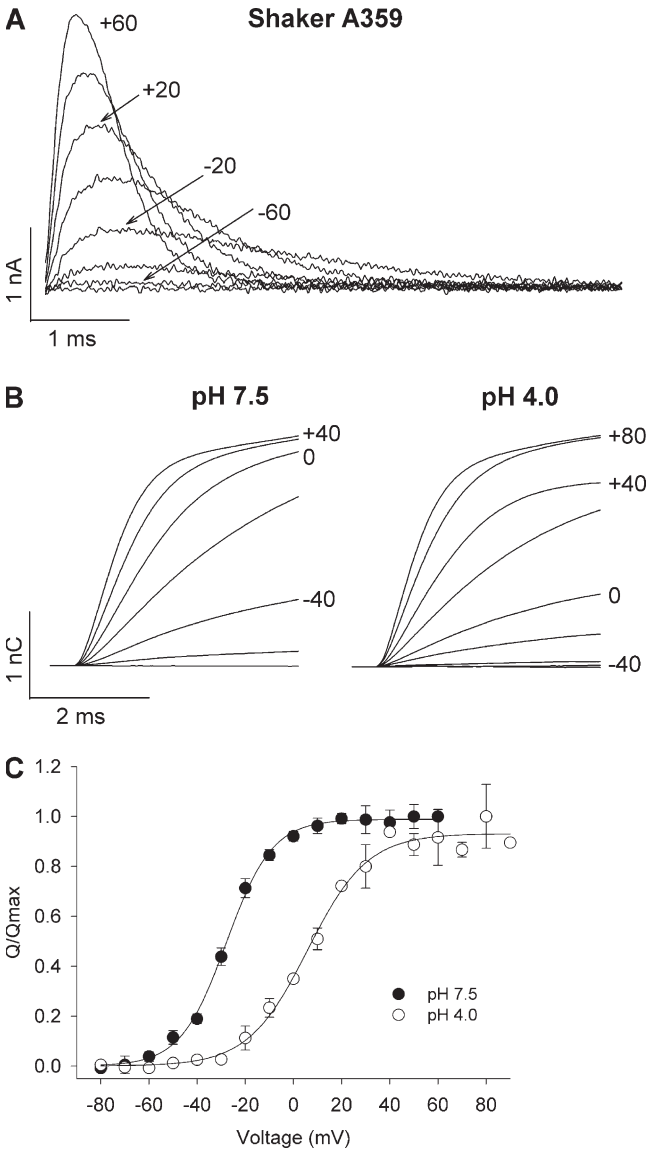

Figure 2. Acidic pH does not alter total gating charge movement in *Shaker* channels. (A) Typical wild-type *Shaker* Δ6–46 (*Shaker* A359) gating current records obtained from *tsa201* cells in the whole-cell patch clamp configuration during 20-ms voltage-clamp pulses from −80 to +60 mV (in 10-mV increments) from a holding potential of −80 mV. Currents during every other pulse are shown for clarity and only the first 6 ms of the depolarizing pulses are shown to highlight the on-gating current. (B) Typical integrals of on-gating currents, such as those in A, recorded in the same cell under control conditions (pH 7.5) and at pH 4.0. Acidic pH did not alter the total gating charge movement in these channels. (C) Mean *Q-V* relationships recorded at pH 7.5 and pH 4.0 (n = 2–4). At pH 4.0, the *Q-V* relation was shifted by ∼+35 mV from −27.9 ± 0.4 mV at pH 7.5 to +5.9 ± 1.2 mV.

labeling of A359C has previously been shown to faithfully report local environmental changes associated with voltage sensor movement in response to membrane depolarization (Mannuzzu et al., 1996; Cha and Bezanilla, 1997). At pH 7.5, there was no obvious channel opening at the holding potential of −80 mV in Fig. 1 B and no voltage sensor movement in Fig. 1 D. On depolarization to −60 mV, despite the low open probability, there was a significant fluorescence report consistent with voltage sensor movement (Fig. 1 D). Further depolarization to +60 mV induced robust ionic currents that activated rapidly and showed only minimal decay (Fig. 1 B). This was reflected in the fluorescence signals (Fig. 1 D), which show a large fluorescence deflection from *Shaker* A359C channels with a fast phase of fluorescence quenching that accounted for 86 ± 2% (n = 8) of the total fluorescence deflection and occurred with a time course similar to that for channel activation. Biexponential fits to the fluorescence relaxation showed that this rapid component was followed by a slow phase that accounted for 14 ± 2% of the deflection and was associated with channel inactivation (Claydon et al., 2006).

At pH 4.0, peak ionic current was reduced by 57 ± 4% (Fig. 1 C; n = 21) even when charge screening was accounted for by the application of a depolarizing pulse to +100 mV, at which open probability was maximal (Fig. 1 A). However, the corresponding fluorescence signals in Fig. 1 E show that the fluorophore continues to report the same extent of environmental change (although with altered kinetics; see below), which suggests that although a proportion of the channels does not conduct at acidic pH, voltage sensor movement is preserved. The mean peak amplitude of the fluorescence deflection at pH 4.0 was 116 ± 11% of that at pH 7.5 (n = 7; t test, not significantly different).

Another measure of voltage sensor movement can be obtained from gating current measurements. We recorded gating currents from wild-type *Shaker* channels at pH 7.5 and pH 4.0 (Fig. 2) and a typical family of records obtained at pH 7.5 during 20-ms voltage-clamp pulses ranging from −80 to +60 mV (the holding potential was −80 mV) is shown in Fig. 2 A (current during the first 6 ms of the pulse is shown to highlight on-gating events). In Fig. 2 B, the integrals of the on-gating currents recorded at pH 7.5 and pH 4.0 in the same cell are plotted. These show that acidic pH shifted the voltage dependence of charge movement to more depolarized potentials, but did not significantly alter the total gating charge movement. This is shown more clearly by the mean *Q-V* relations in Fig. 2 C. Acidic pH shifted the $V_{1/2}$ of the *Q-V* relation by ∼+35 mV from −27.9 ± 0.4 mV (k was 9.5 ± 0.4 mV) at pH 7.5 to +5.9 ± 1.2 mV (k was 12.4 ± 1.0 mV) at pH 4.0, without altering the total gating charge, which suggests that the number of activatable channels (i.e., the number of channels in which the voltage sensors are available to move) is not changed.

It is clear from the fluorescence signals recorded in Fig. 1 E that acidic pH did alter the kinetics of the voltage sensor report. The contribution of the fast phase of the fluorescence signal was reduced to 29 ± 3% of the total signal, because the slow phase was dramatically increased to account for 71 ± 3% of the signal (n = 8; $P < 0.001$,

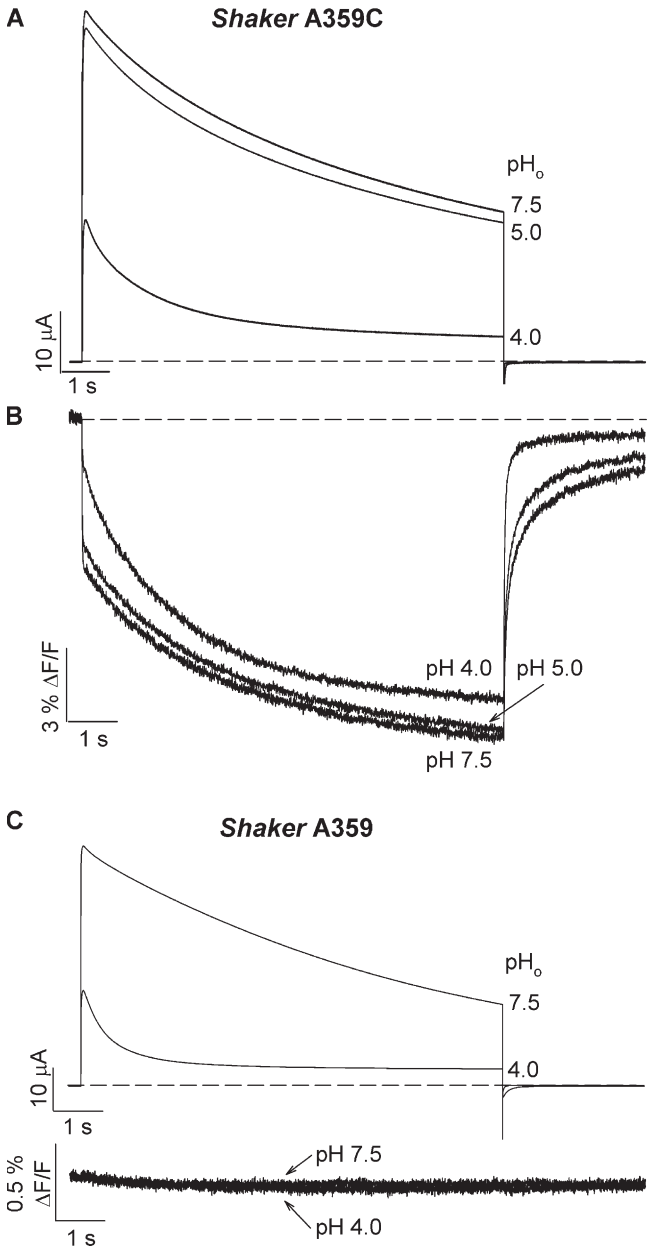

Figure 3. Acidic pH enhances the inactivation report from *Shaker* A359C. Typical ionic currents (A) and fluorescence signals (B) recorded from *Shaker* A359C channels during 7-s voltage-clamp pulses to +60 mV at the indicated external pH (holding potential of −80 mV). (C) Typical ionic currents and fluorescence signals recorded at pH 7.5 and pH 4.0 from TMRM-labeled channels in which a cysteine residue was not engineered at position A359 (*Shaker* A359). These channels lack an externally labelable cysteine residue (the only external cysteine, in the S1–S2 linker [C245], has been removed) and act as a control demonstrating the lack of a voltage-dependent fluorescence deflection in the absence of an introduced cysteine and also the pH independence of emission of the TMRM dye.

paired *t* test, when compared with pH 7.5). Since it has previously been shown that a fluorophore labeling A359C in the S3–S4 linker reports on conformational changes associated with inactivation as well as those associated with voltage sensor movement (Loots and Isacoff, 1998; Claydon et al., 2006), we hypothesized that the enhancement of the slow phase of the fluorescence deflection represented the accelerated onset of inactivation previously reported to occur in *Shaker* channels at low pH (Perez-Cornejo, 1999; Starkus et al., 2003). To test this, we investigated the effect of low pH on the fluorescence report from *Shaker* A359C channels during long depolarizing pulses that induced much more inactivation.

Acidic pH Accelerates the Inactivation Report from *Shaker* A359C Channels

The effect of acidic pH on *Shaker* A359C channel inactivation during 7-s depolarizations to +60 mV is shown in Fig. 3 (see also Table I). The fluorescence signals in Fig. 3 B show a clear slow phase that corresponds to the inactivation of ionic current in panel A. At pH 7.5, ionic current decayed with a τ of 2.7 ± 0.2 s (Fig. 3 A; $n = 14$) and the slow phase of fluorescence decayed with a similar τ of 2.4 ± 0.3 s, and contributed 53 ± 4% to the total signal amplitude (Fig. 3 B; $n = 14$). Reducing the extracellular pH to 5.0 had only a minor effect on ionic current and the fluorescence signal from *Shaker* A359C channels (Figs. 3, A and B). However, pH 4.0 both reduced the peak current amplitude and enhanced the decay of the remaining current (Fig. 3 A; τ was 579 ± 84 ms, $n = 11$). The fluorescence signals in Fig. 3 B, which were recorded simultaneously, show that at pH 4.0 both the contribution and the decay of the slow deflection were enhanced; the contribution of the slow phase was increased to 76 ± 3% and the τ of the slow decay was reduced to 1.2 ± 0.1 s ($n = 14$). These data confirm the previous reports that low pH enhances inactivation of *Shaker* channels (Perez-Cornejo, 1999; Starkus et al., 2003) and suggest that acidic pH enhances the conformational rearrangements associated with inactivation, which are reported by a fluorophore at the outer end of the voltage sensor.

The fluorescence signal recorded from *Shaker* A359C channels returns to baseline upon repolarization and also shows a fast and a slow phase, which represent, respectively, the return of the voltage sensor to its resting conformation during deactivation and the recovery from inactivation (Loots and Isacoff, 1998; Claydon et al., 2006). Both phases were altered by acidic pH (Fig. 3 B); the τ of the fast phase was reduced from 63 ± 16 ms at pH 7.5 to 21 ± 1 ms at pH 4.0 ($n = 17$; $P < 0.05$, paired *t* test), which is consistent with the previous observation that acidic pH accelerates deactivation (Starkus et al., 2003) likely as a result of charge screening, and the τ of the slow phase was reduced from 699 ± 58 ms at pH 7.5 to 202 ± 20 ms at pH 4.0 ($n = 17$; $P < 0.001$, paired *t* test). Since the slow phase of *Shaker* A359C fluorescence return upon repolarization reflects immobilization of the voltage sensor associated with inactivation, it is possible that further slow changes in recovery occur that are beyond the recording period of the experiment.

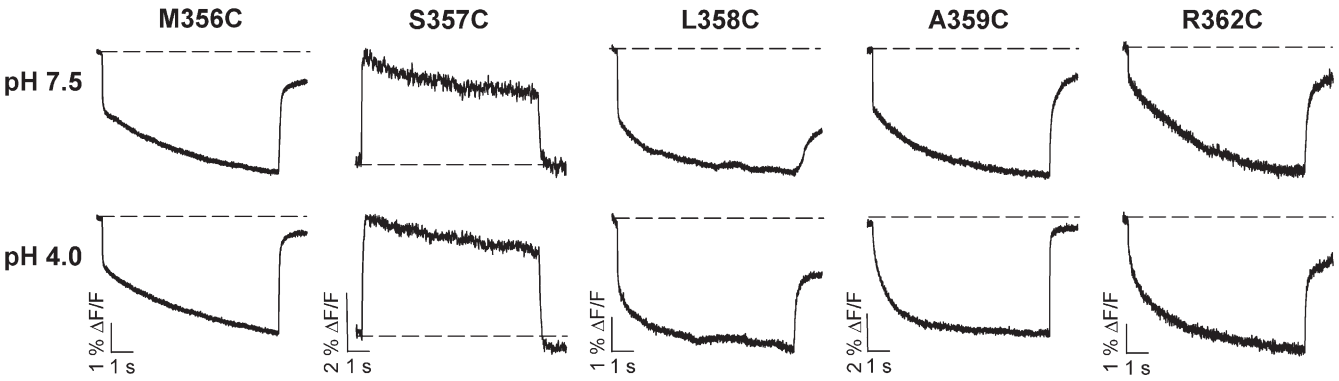

Figure 4. Voltage sensor detection of pH-induced enhancement of inactivation is site specific. Typical fluorescence signals from TMRM attached at different sites in the S4 voltage sensor and S3–S4 linker from M356C to R362C recorded during a 7-s pulse to +60 mV at pH 7.5 and pH 4.0 (holding potential −80 mV). Robust fluorescence deflections were recorded from each site in the scan with the exception of I360C and L361C, from which we were unable to record voltage-dependent fluorescence signals. Only A359C and R362C report the pH-induced enhancement of inactivation.

To demonstrate the specificity of the response of the fluorophore attached at position A359 to changes in external pH, we compared the effect of changing the pH on TMRM-labeled *Shaker* channels lacking an externally labelable cysteine residue (*Shaker* A359; Fig. 3 C and Table I). The decay of ionic current was accelerated from 3.9 ± 0.5 s at pH 7.5 to 0.49 ± 0.07 s at pH 4.0 (n = 3–4; Table I; these values are not significantly different from wild type in the absence of TMRM). The fluorescence signals from *Shaker* A359 demonstrate that there are no voltage-dependent conformational changes reported by TMRM that labels nonspecific sites in endogenous membrane proteins. Furthermore, the fluorescence signal is not altered by changes of the extracellular pH. These results emphasize the ability of site-specific attachment of TMRM to detect gating-induced rearrangements of channel conformation, and in addition, confirm that the emission from TMRM is pH insensitive (Cha and Bezanilla, 1998; see also Molecular Probes website at http://probes.invitrogen.com).

Detection of the pH-induced Acceleration of Inactivation by the Voltage Sensor Is Site Specific

To understand which structural domains are involved in the pH-induced changes in the fluorescence signal from TMRM attached at A359C and the local rearrangements that they represent, we investigated the effect of acidic pH on the fluorescence signal from TMRM attached at each position from M356C in the S3–S4 linker to the outermost arginine, R362C, in the S4 domain. Fluorescence signals recorded during 7-s depolarizing pulses to +60 mV from each of these mutant channels at either pH 7.5 or pH 4.0 extracellular solution are shown in Fig. 4. Each site reported robust fluorescence signals on depolarization with the exception of I360C and L361C, from which only baseline signals could be detected (unpublished data). This lack of signal was unexpected given the fluorescence report from these residues described previously (Loots and Isacoff, 2000). However, we were unable to detect voltage-dependent signals in any of 17 oocytes, which displayed large ionic currents. Close examination of the effect of acidic pH on the fluorescence signal from each mutant channel reveals that only A359C and R362C reported pH-dependent changes. With TMRM attached at R362C, the τ of the slow phase was reduced from 2.6 ± 0.4 s at pH 7.5 to 1.4 ± 0.2 s at pH 4.0 (n = 3; $P < 0.05$, paired t test). Since A359C and R362C are likely positioned on the same side of the S4 helix, this suggests that this face senses the rearrangements associated with the pH modulation of inactivation.

Fluorescence Signals from the Pore Report Two Effects of Acidic pH

Although the fluorescence records from *Shaker* A359C report the rearrangements underlying the acceleration of inactivation at low pH, they do not provide much insight into the basis for the decline of peak current amplitude following extracellular acidification. It has previously been reported that a TMRM fluorophore attached at S424C within the outer pore is a very good reporter of the rearrangements of the *Shaker* channel pore that are associated with inactivation (Loots and Isacoff, 1998). Ionic currents and fluorescence signals recorded from *Shaker* S424C channels in response to 42-s depolarizing pulses to +60 mV at pH 7.5, pH 6.0, and pH 5.0 are shown in Fig. 5. Ionic current at pH 7.5 inactivated with a time constant of 2.0 ± 0.3 s (n = 9; Table I). As in *Shaker* A359C, acidic pH reduced the peak current amplitude and enhanced the decay of the remaining current in *Shaker* S424C channels (Fig. 5 A and Table I) although this mutant channel was more sensitive to acidic pH than *Shaker* A359C as current amplitude was significantly reduced at pH 5.0 (see Fig. 7 A) and ionic current decayed more quickly with a time constant of 264 ± 32 ms (n = 7; Table I). The fluorescence traces in

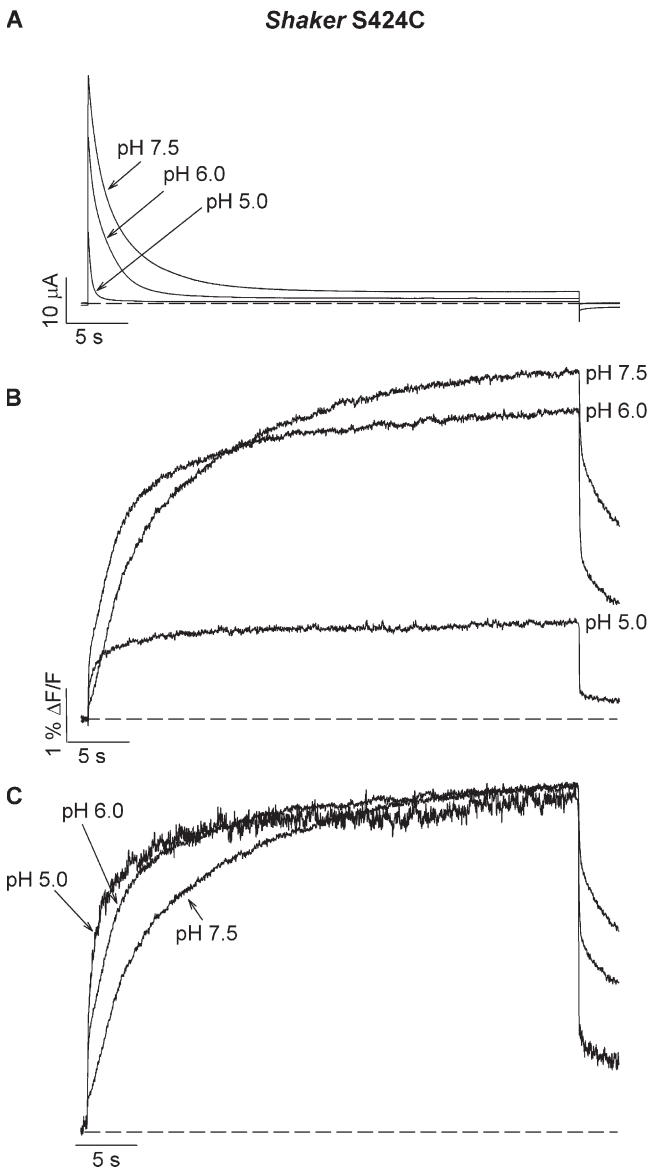

Figure 5. Two effects of acidic pH are detected from TMRM attached within the pore. Typical ionic currents (A) and fluorescence signals (B) recorded from *Shaker* S424C channels during 42-s voltage-clamp pulses to +60 mV at the indicated external pH (holding potential −80 mV). Acidic pH decreased peak and accelerated inactivation of the ionic current, and this was detected in the fluorescence signals as a decrease in the peak fluorescence amplitude and an enhancement of the slow phase of the remaining fluorescence deflection. (C) *Shaker* S424C channel fluorescence deflections from B scaled to the maximum signal amplitude to highlight the pH-induced enhancement of the slow phase of fluorescence deflection.

Fig. 5 B show that TMRM attached at S424C reports the pH-induced inactivation gating modification well. At pH 7.5, the fluorescence signal from *Shaker* S424C shows fast and slow phases on depolarization as reported previously (Loots and Isacoff, 1998; Claydon et al., 2006). The fast phase, reflecting movement of the voltage sensor, was small and contributed only 20 ± 5% of the total signal, whereas the slow phase, representing the conformational rearrangements of the pore during inactivation, contributed 80 ± 5%. The slow phase was best fit with a biexponential function with time constants of 2.6 ± 0.8 and 43.7 ± 22.2 s ($n = 9$). The time constant of the faster component is not significantly different from that of the ionic current decay during P-type inactivation (2.0 ± 0.3 s), while the slower component most likely reflects the slower C-type inactivation process that occurs after ionic current has decayed to baseline. A similar report of C-type inactivation during prolonged depolarization was previously described from the very slow component of fluorescence deflection recorded from A359C (Loots and Isacoff, 1998).

Unlike the report from *Shaker* A359C, the fluorescence signals from *Shaker* S424C at acidic pH demonstrate two effects of protons on channel gating. The first is an acceleration of the slow phase of fluorescence that is consistent with the faster inactivation of ionic current (Fig. 5, A and B). The acceleration of the slow fluorescence report is shown more clearly in Fig. 5 C, which plots the same fluorescence deflections as those in panel B normalized to their peak value. The τ of the faster component of the slow phase was reduced ($n = 5$; $P < 0.05$, paired t test) from 2.6 ± 0.8 s at pH 7.5 to 331 ± 79 ms at pH 5.0 (Table I). The second effect of acidic pH was a decrease of the peak amplitude of the fluorescence signal (Fig. 5 B). Following a transient increase in the fluorescence signal that lasts ~10 s at pH 6.0 (that is due to the acceleration of inactivation upon depolarization and has been described previously, Loots and Isacoff, 1998, for depolarizations of approximately this duration), the fluorescence signal from *Shaker* S424C was reduced by 53 ± 6% at pH 5.0 ($n = 5$) and this was completely restored after returning to pH 7.5 (see Fig. 10 C).

To understand why the macroscopic conductance and the fluorescence report from TMRM at S424C was reduced with acidic pH (Fig. 5), while the report from A359C was not (Figs. 1 and 3), we measured *Shaker-IR* single channel currents at pH 7.4 and pH 4.0 (Fig. 6), since the reduced report from S424C may reflect an effect of protons on channel open probability or the single channel current amplitude. Channel activity was assessed during 500-ms voltage-clamp pulses to +100 mV from outside-out patches (the pulse interval was 15 s). At pH 7.4, the single channel current amplitude (at +100 mV) was 2.7 ± 0.3 pA and the representative traces show high channel availability. We calculated the availability by determining the proportion of sweeps showing channel activity during the first 50 ms of the pulse, and the average availability from 11 patches was 0.87 at pH 7.4. Application of pH 4.0 to the same patch (Fig. 6) markedly reduced availability, resulting in a number of null sweeps (the average availability from five patches was 0.14), but did not alter the single channel current amplitude (2.7 ± 0.3 pA). These data suggest

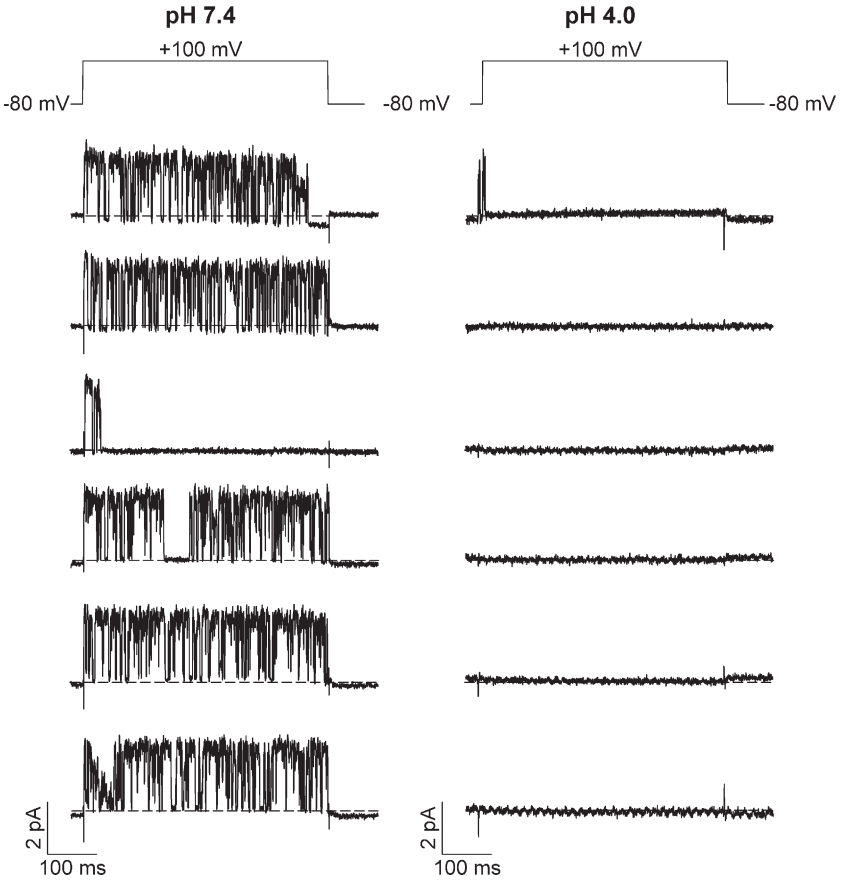

Figure 6. Acidic pH decreases open probability without altering single channel current amplitude. Typical recordings of single channel events obtained from outside-out patches of *ltk−* cells expressing *Shaker* Δ6–46 channels during consecutive 500-ms voltage-clamp pulses to +100 mV (pulse interval 15 s) from a holding potential of −80 mV (the voltage protocol is shown). In this example the patch contains a single channel. Channel activity from the same patch was recorded during control conditions (pH 7.4) and at pH 4.0. Dashed lines mark the zero current level. Acidic pH markedly reduced channel availability (calculated by determining the proportion of sweeps showing channel activity during the first 50 ms of the pulse) from 0.87 at pH 7.4 to 0.14 at pH 4.0 without effect on the single channel current amplitude. At +100 mV, the single channel current amplitude was 2.7 ± 0.3 pA at pH 7.4 and 2.7 ± 0.3 pA at pH 4.0 (data were collected from 11 patches at pH 7.4 and 5 patches at pH 4.0). The 84% reduction in channel availability (from 0.87 to 0.14) was greater than the reduction of macroscopic conductance measured from *Shaker* channels expressed in *Xenopus* oocytes (Fig. 1), but similar to the decrease in peak macroscopic current measured from *Shaker* channels expressed in mammalian cells at pH 4.0 (91 ± 8%; $n = 5$). This difference between expression systems is most likely due to incomplete exchange of solution over the entirety of the large invaginated oocyte membrane.

that the loss of fluorescence observed in Fig. 5 is not due to reduced single channel conductance, but rather reduced channel availability.

Further analysis of the fluorescence data from *Shaker* S424C allowed us to measure the extent of the loss of the fluorescence signal at low pH and show that it was quantitatively correlated to the reduction of peak current amplitude (Fig. 7). Fig. 7 A shows conductance–voltage relationships constructed from *Shaker* S424C currents recorded during 100-ms voltage pulses from −80 to +100 mV at either pH 7.5 or pH 5.0 ($n = 3$). The voltage dependence of the conductance decrease (Fig. 7 A) was compared with the voltage dependence of the pH-induced loss of fluorescence during 42-s voltage pulses (Fig. 7 B) from the same group of oocytes as those in panel A. Long pulses were required to make this comparison, because it was necessary to measure the effect of low pH on the fluorescence amplitude once depolarization-induced inactivation had proceeded to near steady state. In this way the reduction in conductance could be directly compared with the fluorescence report of the proportion of channels that were no longer available to make the transition to the inactivated state.

It is clear that the extent of the loss of fluorescence at pH 5.0 (Fig. 7 B) matches the decrease in conductance (Fig. 7 A) at all potentials. At +60 mV there was a 53 ± 6% loss of the fluorescence signal, which was not significantly different from the 51 ± 3% reduction in conductance ($n = 3$; t test). In Fig. 7 C, the relative fluorescence amplitude at +60 mV is plotted alongside the relative conductance at +60 mV with different external pH. The loss of fluorescence and reduction of conductance showed the same pH dependency with *pKa* values of 5.1 and 5.2, respectively.

The data in Figs. 5–7 demonstrate that acidic pH has two effects: an acceleration of the slow phase of fluorescence from *Shaker* S424C that represents the enhancement of inactivation upon depolarization, and a loss of the fluorescence report from S424C that, in the light of the observed reduction in single channel open probability, suggests a reduction of channel availability and consequently the peak current amplitude. The pH-induced loss of fluorescence signal is of particular interest because it contrasts with the lack of effect of acidic pH on the fluorescence amplitude recorded from *Shaker* A359C channels (Fig. 1 F and Fig. 3 B) and allows a quantitative correlation to be made between the fluorescence loss and conductance decrease at low pH.

Acidic pH Enhances Rearrangements Associated with P- and C-type Inactivation

P/C-type inactivation involves two sequential processes, with a concerted closure of the pore resulting in the collapse of conductance (P-type inactivation) followed

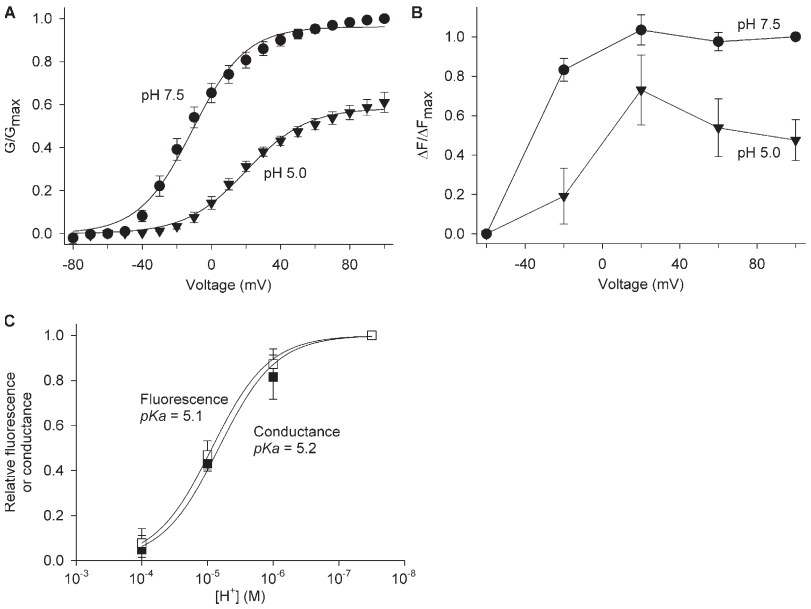

Figure 7. The loss of fluorescence at low pH is similar to the reduction of peak current amplitude. (A) *G-V* relations of *Shaker* S424C channels recorded with the indicated external pH ($n = 3$). Using Eq. 1 (the intracellular K^+ concentration was assumed to be 99 mM), conductance was calculated from currents recorded during 100-ms voltage pulses applied from −80 to +100 mV at 10-s intervals in 10-mV increments (holding potential −80 mV). (B) *F-V* relations of the *Shaker* S424C channels recorded at the indicated pH during 42-s pulses from the same group of oocytes as A ($n = 3$). All fluorescence amplitudes were normalized to the fluorescence amplitude at +100 mV with pH 7.5. Lines represent no mathematical significance and are simply to guide the eye. The loss of fluorescence at low pH was similar to the decrease in conductance at all potentials. (C) Plot of the dependence on the external pH of *Shaker* S424C channel fluorescence amplitude at +60 mV or conductance at +60 mV ($n = 2$–7). Fluorescence and conductance values were normalized to those at pH 7.5. Conductance values were calculated from peak currents recorded at the same time as fluorescence deflections during 42-s pulses so as to directly compare the decrease in conductance with the loss of fluorescence from simultaneous measurements from the same oocyte. Data were fitted with a standard Hill equation (assuming a Hill coefficient, *n*, of 1). *pKa* values were 5.1 and 5.2 for the loss of fluorescence and reduction of conductance, respectively.

by a stabilization of the voltage sensor in its activated conformation (C-type inactivation), which reports as an immobilization of the return of gating charge on repolarization (De Biasi et al., 1993; Olcese et al., 1997; Yang et al., 1997; Loots and Isacoff, 1998). Channels with the mutation W434F are thought to be permanently P-type inactivated (Perozo et al., 1993; Yang et al., 1997), and the fluorescence signal from TMRM attached at S424C in these channels reports well on activation, as if P-type inactivation moves the fluorophore into closer proximity with the voltage sensor and allows it to track the transition of channels to a W434F-like inactivated state (Loots and Isacoff, 1998). This idea is consistent with the close proximity of the S5-P linker with S4 (of an adjacent subunit) in the Kv1.2 channel crystal structure (Long et al., 2005). Since, in the present study, acidic pH accelerates the slow fluorescence report from S424C, this suggests that protons enhance P-type inactivation and we therefore used a protocol designed to monitor the effect of pH on the ability of TMRM attached at S424C to detect voltage sensor movement. Fig. 8 A shows ionic current and fluorescence signals recorded from *Shaker* S424C TMRM-labeled channels during a 2-s test pulse to +60 mV applied either 200 ms, 12 s, or 42 s after a 5-s conditioning pulse to +60 mV. When the interval between pulses was short (200 ms), only a small percentage of channels recovered from inactivation and so the fluorescence signal during the test pulse reports mostly from inactivated channels. In this case, the amplitude of the fast phase of the fluorescence signal was increased from 26 ± 3% in the conditioning pulse to 60 ± 3% during the test pulse ($n = 6$; $P < 0.01$, paired *t* test), suggesting that many channels became P-type inactivated during the conditioning pulse as the fluorophore now reports activation more clearly. With a 42-s interval that allowed for more complete recovery from inactivation, the fluorescence signal during the test pulse recovered its slow phase and the fast phase diminished back to 17 ± 7%. Fig. 8 B shows the effect of acidic pH on the progression of channels to the P-type inactivated state. The double pulse protocol shows that the fast phase dominated during the test pulse at pH 5.0, suggesting that the majority of the channels sense activation well and are therefore P-type inactivated. The contribution of the fast phase in the test pulse after a 200-ms interval at pH 5.0 was 82 ± 4%, which is significantly greater ($n = 5$; $P < 0.01$, paired *t* test) than the 60 ± 3% seen at pH 7.5 (Fig. 8 A). These data demonstrate that the enhancement of current decay at acidic pH is a result of enhanced P-type inactivation.

We next asked whether the progression of channels to the C-type inactivated state could also be altered by changes of pH. To test this, we studied the fluorescence report from TMRM attached at S424C in the presence of the W434F mutation, which permanently P-type inactivates channels (Yang et al., 1997) and allows the rearrangements coupled to C-type inactivation to be observed in isolation. The fluorescence signal shown in Fig. 9 A was recorded during a 7-s pulse to +60 mV at pH 7.5. All signals recorded from this mutant channel were relatively small because the report of the transition to the P-type inactivated state that was evident in Fig. 5 B is absent since W434F mutant channels are P-type

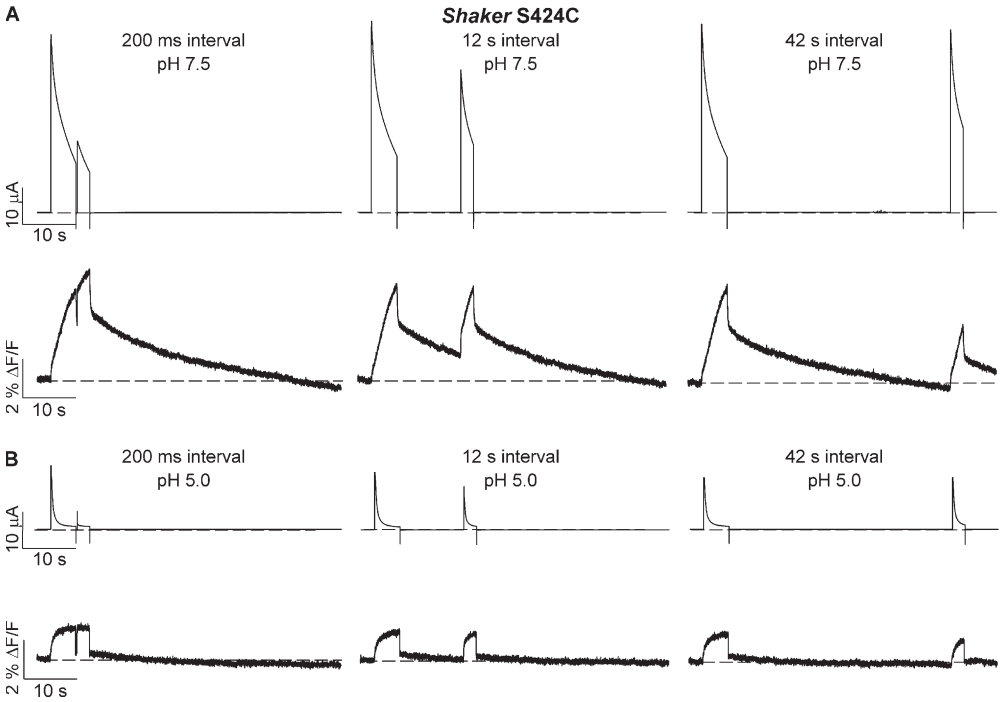

Figure 8. Low pH enhances P-type inactivation. Typical ionic currents and fluorescence signals recorded at pH 7.5 (A) and pH 5.0 (B) from *Shaker* S424C channels during a 2-s test pulse to +60 mV applied either 200 ms, 12 s, or 42 s after a 5-s conditioning pulse to +60 mV (holding potential −80 mV). Similar records were obtained from five other oocytes.

inactivated at rest. There was a prominent fast phase because the P-type inactivated channels reported well on the fast transitions associated with channel activation. Examination of the fluorescence trace in Fig. 9 A shows an additional decaying component of fluorescence, which suggests that a transient reorganization of the pore, sensed by TMRM at S424C, occurs in P-type inactivated channels on depolarization. The amplitude of the decaying component of fluorescence was increased 2.1 ± 0.4-fold at pH 5.0 ($n = 3$; $P < 0.001$, paired *t* test, when compared with pH 7.5). To confirm that this signal represents the progression of channels from the permanent P-type inactivated state to the C-type inactivated state, the voltage dependence of the transition was compared (Fig. 9 B) with that of voltage sensor movement (*Shaker* A359C W434F *F-V*) and the open probability (*Shaker* A359C *G-V*). The C-type inactivation fluorescence–voltage relationship at pH 7.5 (●) and pH 5.0 (○) had $V_{1/2}$ and slope factor, *k*, values of −19.2 ± 2.2 mV and 15.5 ± 1.9 mV, and −21.6 ± 2.1 mV and 19.4 ± 1.8 mV, respectively. For comparison, the peak fluorescence–voltage relation (*F-V*) of *Shaker* A359C W434F channels (▼), which reports the voltage dependence of voltage sensor movement, and the conductance–voltage relation (*G-V*) of *Shaker* A359C channels (▽), which reports the voltage dependence of channel opening, are also plotted in Fig. 9 B. It is clear that the C-type inactivation transition reported by *Shaker* S424C W434F lies to the right of the *Shaker* A359C W434F *F-V* curve and more closely follows the *G-V* relation. This suggests that although the pore is P-type inactivated, the transition to C-type inactivation is dependent on opening of the intracellular gate and not on early independent voltage sensor movements. The data in Fig. 9 B show that this transition is enhanced by acidic pH and, taken together with the data in Figs. 5 and 7, suggest that acidic pH stabilizes both P-type inactivated and C-type inactivated channel states.

The Loss of Fluorescence with Acidic pH Is Determined by Channel Inactivation

The rate of *Shaker* channel inactivation is dependent on the external K^+ concentration. Raising external K^+ increases ion occupancy of the selectivity filter and prevents constriction of the outer pore (Lopez-Barneo et al., 1993). We reasoned that if the mechanistic basis for the loss of fluorescence from S424C with acidic pH was an inactivation process, then raising external K^+ should prevent the changes of fluorescence caused by changing pH. The effect of raising the external K^+ concentration on the fluorescence report from *Shaker* S424C is shown in Fig. 10. In the first set of tracings (Fig. 10 A), the fluorescence emission from *Shaker* S424C channels was recorded during control conditions (pH 7.5, 3 mM external K^+). Application of solution with 3 mM K^+ at pH 5.0 (Fig. 10 B) resulted in a loss of fluorescence as described in Fig. 5, and this was completely reversed on wash with control solution (Fig. 10 C). Solution containing high (99 mM) K^+ was then applied to the same cell (Fig. 10 D). Fig. 10 E shows the effect of acidic pH on the fluorescence in the presence of high external K^+. With 99 mM K^+, pH 5.0 no longer resulted in a loss of the fluorescence signal, suggesting that the loss observed

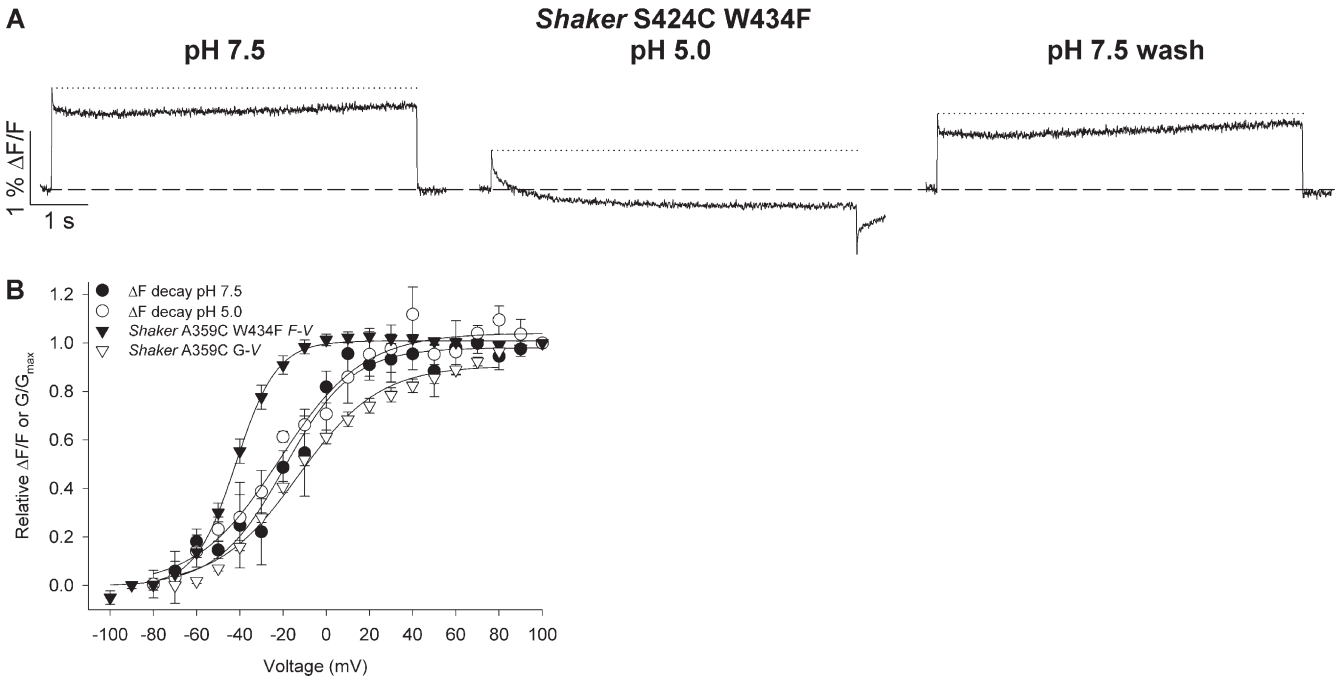

Figure 9. Low pH enhances C-type inactivation. (A) Typical fluorescence signals recorded from the same cell expressing *Shaker* S424C W434F channels during 7-s depolarizing pulses to +60 mV (applied after at least 3 min at the holding potential of −80 mV) at pH 7.5, pH 5.0, and on return to pH 7.5. Oocytes were held at −80 mV for 3 min between measurements. The W434F mutation permanently P-type inactivates channels enabling observation of C-type inactivation rearrangements during depolarizing pulses. The amplitude of the decaying component of fluorescence was approximately twofold larger at pH 5.0 than at pH 7.5. The dotted lines highlight the extent of the decay. The decay of fluorescence was biexponential with τ values of 21 ± 1 ms and 1.8 ± 0.1 s at pH 7.5, and 21 ± 1 ms and 0.36 ± 0.03 s at pH 5.0 ($n = 3$; $P < 0.001$, paired *t* test, when compared with pH 7.5). (B) Plot of the voltage dependence of the amplitude of the decaying component of fluorescence that reflects C-type inactivation ($n = 3$). The amplitude of the decaying component was measured at each potential and normalized to that at +100 mV (ΔF decay). Also plotted is the *G-V* relationship of *Shaker* A359C channels and *F-V* relationship of *Shaker* A359C W434F channels for comparison of the voltage dependence of pore opening and voltage sensor movement, respectively ($n = 5$–21).

with 3 mM K^+ is an inactivation-dependent phenomenon. The increased external K^+ also slowed the decay and largely prevented the reduction of peak ionic current at pH 5.0; the τ of ionic decay was increased from 285 ± 89 ms with 3 mM K^+ at pH 5.0 to 2.9 ± 1.3 s with 99 mM K^+ at pH 5.0, and the peak ionic current was reduced by 51 ± 12% with 3 mM K^+ at pH 5.0, but only by 9 ± 15% with 99 mM K^+ at pH 5.0 ($n = 4$). Responses obtained following wash with pH 7.5 and 3 mM external K^+ are shown in Fig. 10 F.

Inactivation of *Shaker* channels is also largely prevented by the mutation T449V in the outer pore (Lopez-Barneo et al., 1993). Fluorescence signals recorded from *Shaker* S424C T449V with the bath solution adjusted to either pH 7.5 or pH 5.0 are shown in Fig. 11. Neither the amplitude nor rate of decay of the fluorescence emission (Fig. 11) or ionic current (not depicted) on depolarization was altered by application of acidic pH when inactivation was inhibited by the T449V mutation. These data, along with those from the experiments presented in Fig. 10, show that the loss of the fluorescence signal during acidic pH can be prevented in channels when inactivation is compromised.

Acidic pH Induces Conformational Changes in Closed Channels

The fluorescence data presented so far have demonstrated that the environmental changes around TMRM that are associated with both P-type and C-type inactivation are accelerated at low pH (Figs. 3, 5, and 7–9), and the diminished report of TMRM from the pore along with the decreased single channel open probability suggests that protons cause a decrease of channel availability upon depolarization (Figs. 5–7). Further, we have shown that reduction of inactivation prevents this loss of fluorescence at low pH (Figs. 9 and 10). We therefore hypothesized that the loss of fluorescence at acidic pH, and consequently the reduction of channel availability and peak current amplitude, was due to a stabilization of channels in closed-inactivated states. To test this hypothesis, we used the ILT mutant *Shaker* channel (which contains three mutations in the S4 voltage sensor: V369I, I372L, and S376T), as it isolates the early independent voltage sensor movements from the cooperative opening transition of channels (Smith-Maxwell et al., 1998a,b). By applying an appropriate depolarizing pulse amplitude, the effect of acidic pH can be tested on channels in

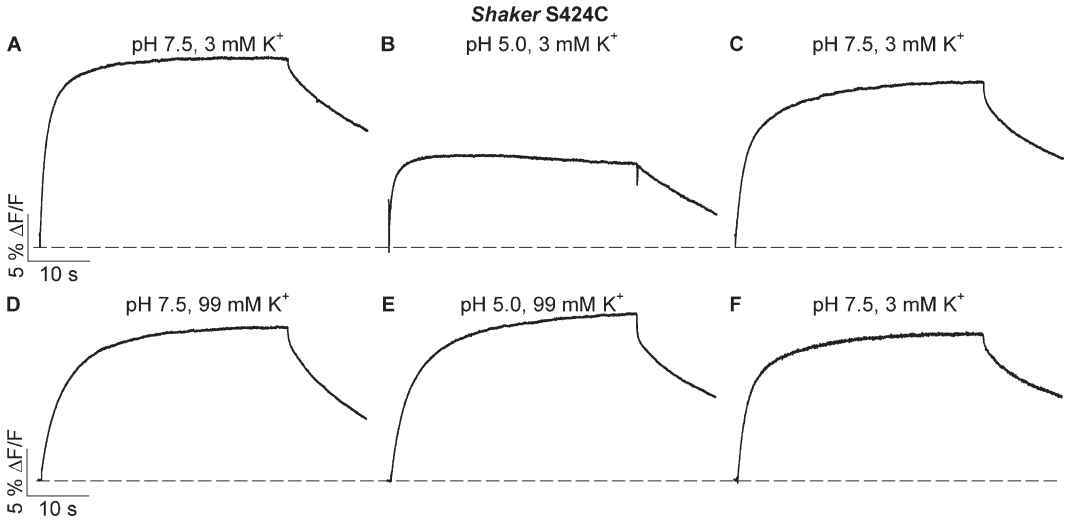

Figure 10. Inhibition of inactivation by raising external K^+ rescues the loss of fluorescence at low pH. (A–F) Typical fluorescence signals recorded from the same oocyte expressing *Shaker* S424C channels during 42-s depolarizing pulses to +60 mV during the indicated manipulations of the external K^+ and proton concentration. After control fluorescence recordings were obtained with 3 mM K^+ and pH 7.5 (A), the pH was reduced to pH 5.0 (with 3 mM K^+) to demonstrate the decrease of fluorescence (B). Fluorescence signals were then recorded on return to pH 7.5 with 3 mM K^+ (C) before application of solution with 99 mM K^+ at pH 7.5 (D). The fluorescence was then measured with 99 mM K^+ and pH 5.0 (E), before the oocyte was washed with control solution (3 mM K^+ and pH 7.5) again (F). Similar records were obtained from three other oocytes.

which the majority of the gating charge has moved, but that still remain closed. Fig. 12 A shows fluorescence records from ILT mutant channels with TMRM attached at S424C during 200-ms depolarizations from −80 to 0 mV. At pH 7.5, the report was small, likely because the fluorophore at S424C does not report well on activation (compare with *Shaker* S424C, Fig. 5), and because the fluorophore does not report the large fluorescence deflection that is associated with inactivation since these channels do not open (at the potentials used in this experiment) and therefore do not make significant transition to the inactivated state. The fluorescence report is reminiscent of gating current recordings from *Shaker* and Kv channels with a fast transient upward fluorescence deflection followed upon repolarization by a slower transient downward fluorescence deflection (Bezanilla et al., 1994; Fedida et al., 1996). At pH 5.0, the fluorescence report from *Shaker* ILT S424C channels was markedly different (Fig. 12 B). In contrast to the weak report at pH 7.5, there was a robust fluorescence deflection with acidic pH that occurred at potentials at which the channels remained closed. Fluorescence deflections in response to voltage pulses from −80 to +80 mV are shown in Fig. 12 B; a stronger depolarization was required because surface charge screening at pH 5.0 shifted activation to more depolarized potentials. In Fig. 12 C, the mean amplitude of the fluorescence deflection from four oocytes at pH 7.5 and pH 5.0 is plotted. It is clear that low pH induced rapid conformational changes that were sensed by the fluorophore in the pore. Furthermore, the pH-induced fluorescence shows a clear voltage dependence that is shifted ∼47 mV to the right of the fluorescence report of voltage sensor movement from *Shaker* ILT A359C W434F channels due to the charge screening effect of protons (the pH-induced shift is similar to that observed in *Shaker* A359C channels in Fig. 1, D and E). In addition, the time constant of the fast phase of fluorescence induced at pH 5.0 in *Shaker* ILT S424C channels displayed a clear voltage dependence that was similar to that of the fast phase in *Shaker* ILT A359C W434F channels at pH 7.5 (Fig. 12 D). These data show that low pH enhances the ability of TMRM

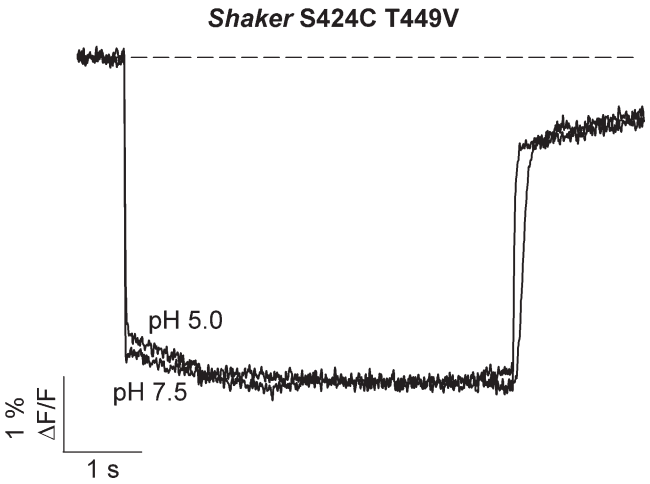

Figure 11. Inhibition of inactivation by the mutation T449V rescues the loss of fluorescence at low pH. Typical fluorescence signals recorded from *Shaker* S424C T449V channels during 7-s depolarizing pulses to +60 mV at pH 7.5 and pH 5.0 (holding potential −80 mV). Inhibition of inactivation prevented the loss of fluorescence at low pH.

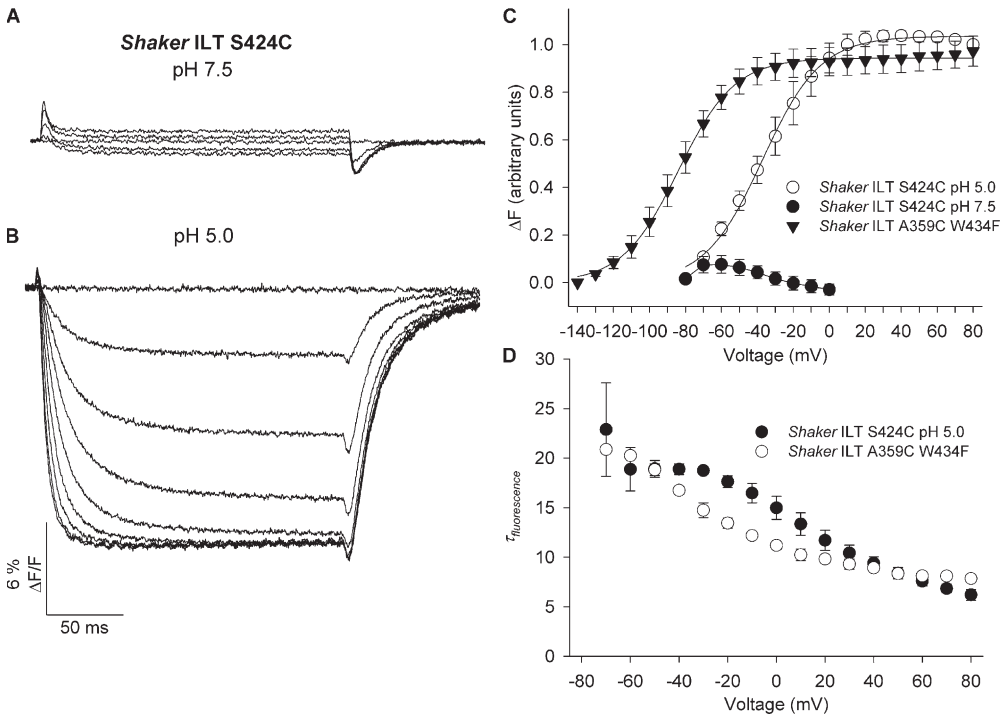

Figure 12. Acidic pH induces conformational changes in closed channels that are associated with inactivation. Typical fluorescence signals recorded from *Shaker* ILT S424C channels during 100-ms voltage pulses from −80 to 0 mV at pH 7.5 (A) and from −80 to +80 mV at pH 5.0 (B). Although pulses were applied in 10-mV increments, only every other pulse is shown for clarity. A voltage pulse to 0 mV at pH 7.5 or to +80 mV at pH 5.0 (shift in voltage dependence is due to surface charge screening by protons) evokes maximum voltage sensor movement without any channel opening. Reduction of the extracellular pH induced conformational changes in closed channels that are consistent with inactivation. (C) Mean *F-V* relationships of the fluorescence recorded from closed channels at pH 7.5 and pH 5.0 from *Shaker* ILT S424C channels ($n = 4$), and from *Shaker* ILT A359C W434F channels ($n = 4$). The $V_{1/2}$ and k values were -37.1 ± 0.8 mV and 16.1 ± 0.7 mV for *Shaker* ILT S424C channels at pH 5.0, and -83.0 ± 0.4 mV and 15.7 ± 0.4 mV for *Shaker* ILT A359C W434F channels at pH 7.5, respectively. (D) Mean τ-V relationships for the fast phase (fitted with a single exponential) of the fluorescence deflection from *Shaker* ILT S424C channels at pH 5.0, and from *Shaker* ILT A359C W434F channels ($n = 4$). The voltage dependence and kinetics of the fluorescence report from *Shaker* ILT S424C channels was similar to that of voltage sensor movement reported by *Shaker* A359C W434F.

attached at S424C to detect the rapid activation movements of the voltage sensor on depolarization in channels that remain closed, and therefore suggest that acidic pH induces a W434F-like inactivated conformation of the pore in closed channels.

Another direct demonstration of closed-state rearrangements at low pH is shown in Fig. 13. The diary plot in Fig. 13 A shows fluorescence emission from *Shaker* ILT S424C channels sampled at 5-s intervals while holding channels at −80 mV and changing the pH of the solution. The fluorescence emission from closed channels was clearly altered by the pH. Fig. 13 B shows a plot of the mean relative fluorescence change from that at pH 7.5 at each pH in three oocytes. The fluorescence deflection was 112 ± 2, 111 ± 2, 105 ± 2, and $100 \pm 3\%$ that of the deflection at pH 7.5 during exposure to pH 4.0, 5.0, 6.0, and 8.0, respectively ($n = 3$). The pH dependence of the closed-state rearrangements had a *pKa* of 5.9, which is similar to that reported above for the pH dependence of the loss of the fluorescence and the conductance decrease (pH 5.1 and 5.2, respectively). Similar changes of pH had no effect on the fluorescence emission of TMRM-treated *Shaker* channels that lack an external cysteine (*Shaker* A359, Fig. 13 C). These data demonstrate that low pH induces conformational rearrangements in closed channels that are detected by S424C and taken together with the data presented above suggest that acidic pH induces inactivation-dependent conformational rearrangements of channels while they reside in closed states.

DISCUSSION

Loss of Conductance at Low pH

The fluorescence results presented here support the idea that acidic pH stabilizes both open- and closed-inactivated channel states. Upon depolarization, low pH accelerates inactivation from the open state (depolarization-induced inactivation), which is manifest as an enhancement of the rate of decay of ionic current and of the fluorescence report of P- and C-type inactivation in *Shaker* A359C and *Shaker* S424C channels (Figs. 1, 3–5, and 8–11), as discussed below. However, this is not the major mechanism by which peak current is reduced. Instead, our fluorescence studies demonstrate that low pH also induces inactivation of channels from resting closed states, which is manifest as the loss of the fluorescence signal in *Shaker* S424C channels and the decrease in peak current amplitude (Figs. 5 and 7–13). We propose that the loss of fluorescence reports the decrease of conductance seen in Fig. 1 A and Fig. 7 A as it is clear from the report from A359C (Fig. 1, D and E) and the gating current measurements (Fig. 2 C) that the number

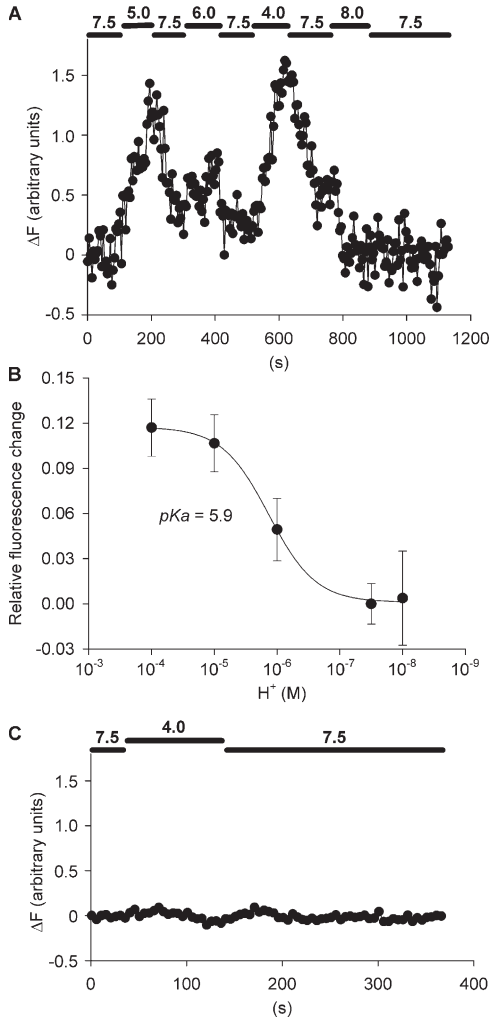

Figure 13. Demonstration of pH-induced closed-state rearrangements. Typical diary plots of the effect of changing the pH on the fluorescence emission from *Shaker* ILT S424C (A) or *Shaker* A359 (C, as a control) channels held continuously at −80 mV. To minimize bleaching of the fluorophore, fluorescence was sampled every second (although only every fifth recording is shown for clarity) by opening the shutter for 100 ms. Low pH induced rearrangements at −80 mV that were detected by TMRM at S424C. (B) Plot of the dependence of the closed-state fluorescence changes on the external pH (n = 3). The relative fluorescence change from that at pH 7.5 is plotted. Data were fitted with a standard Hill equation (assuming a Hill coefficient, n, of 1). The *pKa* for the closed-state fluorescence change was pH 5.9. The value at pH 7.5 represents the mean of all pre- and post-treatment conditions since the order of pH changes was not necessarily consistent.

of activatable channels was not altered by acidic pH (i.e., total gating charge movement was not reduced by protons) and there is no evidence from the single channel recordings that external protons reduce single *Shaker* channel current amplitude (Fig. 6). It is possible that the fluorophores in a proportion of the channels no longer report during exposure to acidic pH because they have moved into a position that no longer senses the collapse of the pore during depolarization-induced inactivation. However, the loss of fluorescence was prevented by interventions that inhibited inactivation, such as raising the external K^+ concentration (Fig. 10) and the mutation T449V (Fig. 11), which indicates that this population of channels no longer report simply because the channels are already inactivated. In agreement with this, use of the ILT mutant channel to isolate voltage sensor movement from pore opening (Smith-Maxwell et al., 1998a,b) demonstrates that, at potentials at which channels do not open, low pH induces fluorophore movement into a position from which it better detects voltage sensor movement (Fig. 12). The improved report of activation on going from pH 7.5 to pH 5.0 suggests that, even though these channels do not open (at the test potential used), acidic pH stabilizes an inactivated W434F-like conformation and this is consistent with the decreased single channel availability observed in Fig. 6. In support of this, we were able to directly observe conformational rearrangements in channels held at −80 mV when the pH of the solution was lowered (Fig. 13).

It is interesting that the large fluorescence deflection observed with *Shaker* ILT S424C (Fig. 12) was not observed in *Shaker* S424C channels at low pH (Fig. 5). Those channels that are closed inactivated should report a rapid fluorescence deflection on depolarization, but this is not evident. This may be because this report is masked by the robust signal from open and inactivating *Shaker* S424C channels at low pH. Indeed, Fig. 9 A shows that permanently inactivated *Shaker* S424C channels produce only a small fluorescence deflection (see also Fig. 4 C in Loots and Isacoff, 1998). It appears that the ILT mutation can enhance the report of activation in channels that are closed-state inactivated in some way that is not fully understood at the present time.

A positive correlation between the rate of depolarization-induced P/C-type inactivation and the prevalence of closed-state inactivation has been reported previously (Lopez-Barneo et al., 1993). These authors showed that reducing external K^+ reduced channel availability (i.e., decreased the proportion of channels able to conduct ions on depolarization) more significantly in mutant *Shaker* channels that displayed accelerated depolarization-induced inactivation. This conclusion is also supported by the demonstration that the loss of fluorescence and the decrease of macroscopic conductance share a very similar pH dependence with *pKa* values of 5.1 and 5.2, respectively (Fig. 7), and is consistent with the observation that low pH markedly reduced the open probability of *Shaker* single channels (Fig. 6). Similar findings are reported for the effect of acidic pH on Kv1.5 channels in which single channels switch between available and unavailable states (Kwan et al., 2006). This predicts the loss of the macroscopic fluorescence signal and maximal conductance that we observe since these measurements represent the proportion of channels that are in

the unavailable state. Our fluorescence data from *Shaker* channels demonstrate that the *pKa* for the transition to the unavailable closed-inactivated state is pH 5.1–5.9 (Fig. 7 C and Fig. 13 B). The *pKa* values for the stabilization of closed-state inactivation and loss of conductance (pH 5.2, Fig. 7 C) are similar to previously reported *pKa* values, pH 4.7–5.0, for the effect of protons on P/C-type inactivation from the open state (Perez-Cornejo, 1999; Starkus et al., 2003). In Kv1.5 channels, the *pKa* values for the inhibition of maximal conductance and the acceleration of inactivation by external acidification only differ by 0.3 pH units (*pKa* = pH 6.2 and pH 6.5, respectively; unpublished data). This suggests that the effects of acidic pH on closed- and open-state inactivation may involve the same mechanism.

An argument against this idea is the differential sensitivity of pH-induced closed- and open-state inactivation to external K^+. For example, raising external K^+ from 3 to 99 mM completely reversed the loss of the fluorescence signal caused by acidic pH, suggesting that 99 mM K^+ prevents closed-state inactivation entirely (Fig. 10). However, the report of P/C-type inactivation was only slowed approximately twofold (from 2.0 ± 0.6 to 3.6 ± 0.4 s; $n = 3$) and not completely prevented (Fig. 10). Differential sensitivities of P/C-type inactivation and the inhibition of maximal conductance by acidic pH to external K^+ are also evident in Kv1.5 channels (Fedida et al., 1999; Zhang et al., 2005). However, this difference is probably due to the fact that the K^+-sensitive site in the pore that mediates inactivation is flooded by efflux of internal K^+ in open channels such that it is relatively insensitive to changes in external K^+, whereas the absence of K^+ efflux in closed channels reveals the sensitivity of inactivation to the external K^+ concentration, as is the case with depolarization-induced inactivation in the presence of an internal pore blocker or with the removal of internal K^+ (Baukrowitz and Yellen, 1995).

Enhancement of P-type Inactivation at Low pH

It is well established that acidic extracellular pH enhances the rate of inactivation upon depolarization in a number of Kv channels, such as *Shaker*, Kv1.4, and Kv1.5, although their sensitivity to protons differs (Steidl and Yool, 1999; Claydon et al., 2000; Kehl et al., 2002; Starkus et al., 2003). Our fluorescence studies enable direct observation of the rearrangements associated with the collapse of the pore during P-type inactivation from the report of TMRM attached either within the pore at S424C or at the top of the voltage sensor at A359C. Acidic pH enhanced the slow phase of the fluorescence report from TMRM attached at A359C and at S424C that reports the dynamic structural changes associated with P-type inactivation (Fig. 3 B and Fig. 5 B). In addition, the experiments in Fig. 6 suggest that a greater proportion of channels make the transition at rest to the W434F-like P-type inactivated state at pH 5.0 than at pH 7.5. These findings are consistent with the enhanced decay of current seen in Fig. 3 A and Fig. 5 A and also with data from previous studies during exposure to acidic pH (Claydon et al., 2002; Kehl et al., 2002; Starkus et al., 2003; Zhang et al., 2003), as well as the enhanced decay of fluorescence that was previously observed from TMRM attached at S424C (Loots and Isacoff, 1998).

Enhancement of C-type Inactivation at Low pH

W434F mutant channels are thought to be permanently P-type inactivated (Perozo et al., 1993; Yang et al., 1997), and therefore transitions to the C-type inactivated state should be observable on depolarization from a fluorophore placed in the outer pore. Our fluorescence records from TMRM attached at S424C in W434F mutant channels (Fig. 9 A) showed a large fast deflection consistent with previous fluorescence observations in this channel (Loots and Isacoff, 1998) and also the notion that the fluorophore in P-type inactivated channels occupies a position that senses the movement of the voltage sensors very well (Loots and Isacoff, 1998). However, in addition to the rapid fluorescence deflection, we observed a secondary fluorescence deflection that most likely represents the progression of channels to the C-type inactivated state, and this was enhanced during acidic pH (Fig. 9, A and B). The C-type inactivation fluorescence transition was best fit with a double exponential function, and although the mechanistic basis for this is uncertain, only the slower time constant was reduced by acidic pH. The voltage dependence of the total amplitude of the fluorescence deflection followed that expected for channel opening (Fig. 9 C). This suggests that, although these channels are permanently P-type inactivated, activation of the voltage sensors is not sufficient to cause C-type inactivation, and that transition to the C-type inactivated state can only occur once the intracellular gate opens. Furthermore, this suggests that, unlike P-type inactivation, C-type inactivation cannot occur from resting closed states.

Although we have demonstrated a clear secondary fluorescence deflection that probably reflects C-type inactivation, it was not evident in the previous report of fluorescence from S424C in W434F mutant channels (Loots and Isacoff, 1998). This could be due to an additional mutation (C462A) made in those studies, which enhanced the rate of inactivation ~20-fold (Loots and Isacoff, 1998) and perhaps made the transition to C-type inactivation too rapid to resolve.

A Discrete Site in S4 Reports the pH-induced Alteration of Inactivation

It has previously been suggested that the S4 domain moves close to, and even interacts with, the S5-P linker in an adjacent subunit of the channel (Blaustein et al., 2000; Elinder et al., 2001; Gandhi et al., 2000; Larsson and Elinder, 2000; Li-Smerin et al., 2000; Loots and

Isacoff, 2000; Ortega-Saenz et al., 2000; Lainè et al., 2003; Long et al., 2005) and that TMRM attached at A359C at the top of the voltage sensor reports inactivation gating rearrangements (Loots and Isacoff, 1998, 2000; Gandhi et al., 2000; Long et al., 2005; Claydon et al., 2006). It is clear from the present study that A359C and R362C are unique amongst sites in the S3–S4 linker and at the top of S4 in their ability to sense the pH-induced enhancement of inactivation (Fig. 4). In a previous comprehensive scan of the extracellular domains of the *Shaker* channel (Gandhi et al., 2000) it was demonstrated that all sites from M356C to R362C report on inactivation of the pore and that TMRM at sites within the outer portion of the helical S4 domain can sense inactivation rearrangements regardless of their orientation (Loots and Isacoff, 2000). Our results are generally consistent with these (except that we could not record deflections from either I360C or L361C); however, the data in Fig. 4 suggest that only two of these sites, which are adjacent to each other on the same side of the S4 α-helix that faces the pore, sense the pH-induced changes (although we cannot exclude that I360C and L361C might sense such changes). It is unclear why we were unable to record fluorescence deflections from I360C and L361C (even with oocytes expressing >200 μA of current) that were reported by Loots and Isacoff (2000). Since these authors suggest that these two sites report only on inactivation (because the fluorescence signal is dominated by a slow component and there is little evidence of a fast component on the same time scale as activation), it is possible that their inclusion of the mutation C462A is the reason for the discrepancy. This mutation is known to speed inactivation ~20-fold (Loots and Isacoff, 1998) and the report of inactivation in this background would therefore be expected to be much more pronounced.

Our data suggest either that the inactivation gating rearrangements that are induced at low pH are localized so that they are only sensed by this region or that protons alter the interaction of S4 with the pore and, as a consequence, the influence of inactivation on TMRM attached in S4. Further studies are clearly required to address the effect of pH on the dynamic interaction of S4 with the pore.

It has been suggested that the extent of fluorescence quenching of TMRM attached at A359C is increased with acidic pH (Cha and Bezanilla, 1997; Sorensen et al., 2000), an effect that was attributed to the protonation of a titratable group within the S3–S4 linker. In the present study, we observed a trend for the fluorescence deflection to increase in amplitude during application of acidic pH, although the data did not reach statistical significance (Fig. 1, D and E). However, the key observation was that the fluorescence amplitude from *Shaker* A359C was not reduced during acidic pH (Fig. 1, D and E). The lack of reduction of the signal strongly suggests that the total gating charge movement was not altered by external protons and is consistent with the observation that acidic pH did not alter the amplitude of on-gating charge movement (Fig. 2 C). Clearly, the kinetics of the report of channel gating are dramatically altered during acidic pH (Fig. 1, D and E), but we do not interpret this as a reduction in the gating charge movement, given that the total signal amplitude is unchanged, but rather that the enhancement of the inactivation report masks the report of activation. This suggests that although the pore reports a loss of channel availability at low pH, the number of activatable channels is not reduced.

Other Channels and Other Mechanisms

In Kv1.5 channels, although the *pKa* for the inhibition by protons is ~pH 6.2 with 2–5 mM external K^+ (Steidl and Yool, 1999; Kehl et al., 2002), lowering the pH to 5.5 results in a loss of conductance of channels in which the histidine, which acts as a pH sensor in the outer pore, has been mutated to glutamine (H463Q; Kehl et al., 2002). This suggests that there are two titratable sites in the Kv1.5 pore, one that has a *pKa* of ~pH 6.2 and, when protonated, enhances inactivation, and a second that has a lower *pKa*, which, when protonated, causes a loss of macroscopic conductance. The *Shaker* channel lacks the histidine pH sensor, and current is inhibited with a *pKa* of ~pH 4.0–5.0 (Perez-Cornejo, 1999; Starkus et al., 2003; see also Fig. 1 A), leading to the suggestion that D447 in the outer pore may act as the pH sensor (Starkus et al., 2003). Since this residue is conserved in Kv1.5 channels, this site may also act as the low range pH sensor that regulates availability in these channels. Consistent with this idea, mutations of *Shaker* D447 accelerate inactivation (D447E) or alter current level (D447N) (Molina et al., 1998).

It is known that Kv channels, once inactivated, become significantly more permeable to Na^+ (Starkus et al., 1997; Wang et al., 2000), and this has been used as another way to examine transitions between inactivated states at low pH (Zhang et al., 2003). Many of the observations made on Na^+ currents through inactivated Kv channels support the conclusions made from the fluorescence data obtained from *Shaker* channels described here. In the Na^+ experiments there was a large decrease in open-state current at low pH, but large slow inward Na^+ tail currents were maintained upon repolarization. This supports the idea that channels can still activate and deactivate at low pH without passing through the open state, and thus activation gating is expected to be maintained. This is supported by the gating current measurements in Fig. 2 as well as the fluorescence experiments in Figs. 1 and 3, which imply that low pH does not alter total gating charge movement. As well, these Na^+ permeation experiments showed an equivalent Na^+ conductance through open-inactivated channels during sustained

depolarizations at normal and acidic pH. These data suggest the possibility that channels are closed-inactivated at low pH, and are able to activate directly into Na^+-conductive depolarization-induced inactivated states without actually opening. This idea is consistent with the present fluorescence and single channel experiments, which show directly that a population of channels becomes unavailable during acidic pH (Figs. 5, 6, and 10) due to the stabilization of inactivation from resting closed channel states (Figs. 10–13), making them unable to open. A kinetic model to describe the Na^+ permeation experiments suggested that channels accumulated in the open-inactivated state during depolarization and made the transition to closed-inactivated states via an intermediate "R" state in the recovery pathway (Zhang et al., 2003). Channels could not reopen from resting closed-inactivated states in the model (Zhang et al., 2003), but it is not clear whether or not Na^+ as the permeant ion causes other structural changes within the selectivity filter that do not allow it to accurately model activation of closed-inactivated channels with K^+ as the charge carrier (Panyi and Deutsch, 2006).

It has previously been shown that *Shaker* channels may undergo a type of closed-state inactivation called U-type inactivation (Klemic et al., 2001) and it is helpful to consider whether this is the closed state stabilized at low pH. In U-type inactivation, maximal current reduction occurs at intermediate potentials, where the dwell time in intermediate states is longer, and less inactivation occurs at more depolarized potentials when the open probability is high, resulting in a characteristic U-shaped inactivation–voltage relationship. However, although the fluorescence data strongly support closed-state inactivation, the effects of raising external K^+ reported here are opposite to those expected for U-type inactivation. U-type inactivation is enhanced by raising external K^+ (Klemic et al., 2001), whereas we show in Fig. 10 that high external K^+ rescues channels from closed-state inactivation, which suggests that the pH-induced closed-state inactivation is unlikely to be U-type in nature.

This work was supported by grants from the Heart and Stroke Foundation of British Columbia and Yukon and the Canadian Institutes of Health Research to D. Fedida and S.J. Kehl. D. Fedida is supported by a Career Investigator award from the Heart and Stroke Foundation of British Columbia and Yukon. T.W. Claydon was supported by a postdoctoral research fellowship funded by a Focus on Stroke strategic initiative from The Canadian Stroke Network, the Heart and Stroke Foundation, the CIHR Institute of Circulatory and Respiratory Health, and the CIHR/Rx&D Program along with AstraZeneca Canada. M. Vaid was supported by a Michael Smith Foundation for Health Research Studentship. S. Rezazadeh was supported by a Heart and Stroke Foundation of British Columbia and Yukon Studentship and a University of British Columbia Graduate Fellowship.

Olaf S. Andersen served as editor.

Submitted: 2 March 2007
Accepted: 6 April 2007

REFERENCES

Baukrowitz, T., and G. Yellen. 1995. Modulation of K^+ current by frequency and external $[K^+]$: a tale of two inactivation mechanisms. *Neuron.* 15:951–960.

Bezanilla, F. 2002. Voltage sensor movements. *J. Gen. Physiol.* 120:465–473.

Bezanilla, F., E. Perozo, and E. Stefani. 1994. Gating of *Shaker* K^+ channels: II. The components of gating currents and a model of channel activation. *Biophys. J.* 66:1011–1021.

Blaustein, R.O., P.A. Cole, C. Williams, and C. Miller. 2000. Tethered blockers as molecular 'tape measures' for a voltage-gated K^+ channel. *Nat. Struct. Biol.* 7:309–311.

Cha, A., and F. Bezanilla. 1997. Characterizing voltage-dependent conformational changes in the *Shaker* K^+ channel with fluorescence. *Neuron.* 19:1127–1140.

Cha, A., and F. Bezanilla. 1998. Structural implications of fluorescence quenching in the *Shaker* K^+ channel. *J. Gen. Physiol.* 112:391–408.

Claydon, T.W., M.R. Boyett, A. Sivaprasadarao, K. Ishii, J.M. Owen, H.A. O'Beirne, R. Leach, K. Komukai, and C.H. Orchard. 2000. Inhibition of the K^+ channel Kv1.4 by acidosis: protonation of an extracellular histidine slows the recovery from N-type inactivation. *J. Physiol.* 526:253–264.

Claydon, T.W., M.R. Boyett, A. Sivaprasadarao, and C.H. Orchard. 2002. Two pore residues mediate acidosis-induced enhancement of C-type inactivation of the Kv1.4 K^+ channel. *Am. J. Physiol. Cell. Physiol.* 283:C1114–C1121.

Claydon, T.W., M. Vaid, S. Rezazadeh, S.J. Kehl, and D. Fedida. 2006. 4-Aminopyridine prevents the conformational changes associated with P/C-type inactivation in *Shaker* channels. *J. Pharmacol. Exp. Ther.* 320:162–172.

De Biasi, M., H.A. Hartmann, J.A. Drewe, M. Taglialatela, A.M. Brown, and G.E. Kirsch. 1993. Inactivation determined by a single site in K^+ pores. *Pflugers Arch.* 422:354–363.

Deutsch, C., and S.C. Lee. 1989. Modulation of K^+ currents in human lymphocytes by pH. *J. Physiol.* 413:399–413.

Elinder, F., R. Mannikko, and H.P. Larsson. 2001. S4 charges move close to residues in the pore domain during activation in a K channel. *J. Gen. Physiol.* 118:1–10.

Fedida, D., R. Bouchard, and F.S. Chen. 1996. Slow gating charge immobilization in the human potassium channel Kv1.5 and its prevention by 4-aminopyridine. *J. Physiol.* 494:377–387.

Fedida, D., N.D. Maruoka, and S. Lin. 1999. Modulation of slow inactivation in human cardiac Kv1.5 channels by extra- and intracellular permeant cations. *J. Physiol.* 515:315–329.

Gandhi, C.S., E. Loots, and E.Y. Isacoff. 2000. Reconstructing voltage sensor-pore interaction from a fluorescence scan of a voltage-gated K^+ channel. *Neuron.* 27:585–595.

Hille, B. 2001. Classical mechanisms of block. *In* Ion channels of excitable membranes. Sinauer Associates Inc., Sunderland, MA. 503–538.

Hoshi, T., W.N. Zagotta, and R.W. Aldrich. 1991. Two types of inactivation in *Shaker* K^+ channels: effects of alterations in the carboxy-terminal region. *Neuron.* 7:547–556.

Jäger, H., and S. Grissmer. 2001. Regulation of a mammalian *Shaker*-related potassium channel, hKv1.5, by extracellular potassium and pH. *FEBS Lett.* 488:45–50.

Kehl, S.J., C. Eduljee, D.C. Kwan, S. Zhang, and D. Fedida. 2002. Molecular determinants of the inhibition of human Kv1.5 potassium currents by external protons and Zn^{2+}. *J. Physiol.* 541:9–24.

Klemic, K.G., G.E. Kirsch, and S.W. Jones. 2001. U-type inactivation of Kv3.1 and *Shaker* potassium channels. *Biophys. J.* 81:814–826.

Kurata, H.T., and D. Fedida. 2006. A structural interpretation of voltage-gated potassium channel inactivation. *Prog. Biophys. Mol. Biol.* 92:185–208.

Kwan, D.C., D. Fedida, and S.J. Kehl. 2006. Single channel analysis reveals different modes of Kv1.5 gating behavior regulated by changes of external pH. *Biophys. J.* 90:1212–1222.

Lainè, M., M.C. Lin, J.P. Bannister, W.R. Silverman, A.F. Mock, B. Roux, and D.M. Papazian. 2003. Atomic proximity between S4 segment and pore domain in *Shaker* potassium channels. *Neuron.* 39:467–481.

Larsson, H.P., and F. Elinder. 2000. A conserved glutamate is important for slow inactivation in K^+ channels. *Neuron.* 27:573–583.

Li-Smerin, Y., D.H. Hackos, and K.J. Swartz. 2000. α-helical structural elements within the voltage-sensing domains of a K^+ channel. *J. Gen. Physiol.* 115:33–50.

Long, S.B., E.B. Campbell, and R. MacKinnon. 2005. Voltage sensor of Kv1.2: structural basis of electromechanical coupling. *Science.* 309:903–908.

Loots, E., and E.Y. Isacoff. 2000. Molecular coupling of S4 to a K^+ channel's slow inactivation gate. *J. Gen. Physiol.* 116:623–636.

Loots, E., and E.Y. Isacoff. 1998. Protein rearrangements underlying slow inactivation of the *Shaker* K^+ channel. *J. Gen. Physiol.* 112:377–389.

Lopez-Barneo, J., T. Hoshi, S.H. Heinemann, and R.W. Aldrich. 1993. Effects of external cations and mutations in the pore region on C-type inactivation of *Shaker* potassium channels. *Receptors Channels.* 1:61–71.

Mannuzzu, L.M., M.M. Moronne, and E.Y. Isacoff. 1996. Direct physical measure of conformational rearrangement underlying potassium channel gating. *Science.* 271:213–216.

Molina, A., P. Ortega-Saenz, and J. Lopez-Barneo. 1998. Pore mutations alter closing and opening kinetics in *Shaker* K^+ channels. *J. Physiol.* 509:327–337.

Olcese, R., R. Latorre, L. Toro, F. Bezanilla, and E. Stefani. 1997. Correlation between charge movement and ionic current during slow inactivation in *Shaker* K^+ channels. *J. Gen. Physiol.* 110:579–589.

Ortega-Saenz, P., R. Pardal, A. Castellano, and J. Lopez-Barneo. 2000. Collapse of conductance is prevented by a glutamate residue conserved in voltage-dependent K^+ channels. *J. Gen. Physiol.* 116:181–190.

Panyi, G., and C. Deutsch. 2006. Cross talk between activation and slow inactivation gates of *Shaker* potassium channels. *J. Gen. Physiol.* 128:547–559.

Perez-Cornejo, P. 1999. H^+ modulation of C-type inactivation of *Shaker* K^+ channels. *Pflugers Arch.* 437:865-870.

Perozo, E., R. MacKinnon, F. Bezanilla, and E. Stefani. 1993. Gating currents from a nonconducting mutant reveal open-closed conformations in *Shaker* K^+ channels. *Neuron.* 11:353–358.

Smith-Maxwell, C.J., J.L. Ledwell, and R.W. Aldrich. 1998a. Role of the S4 in cooperativity of voltage-dependent potassium channel activation. *J. Gen. Physiol.* 111:399–420.

Smith-Maxwell, C.J., J.L. Ledwell, and R.W. Aldrich. 1998b. Uncharged S4 residues and cooperativity in voltage-dependent potassium channel activation. *J. Gen. Physiol.* 111:421–439.

Somodi, S., Z. Varga, P. Hajdu, J.G. Starkus, D.I. Levy, R. Gaspar, and G. Panyi. 2004. pH-dependent modulation of Kv1.3 inactivation: the role of His399. *Am. J. Physiol. Cell Physiol.* 287: C1067–C1076.

Sorensen, J.B., A. Cha, R. Latorre, E. Rosenman, and F. Bezanilla. 2000. Deletion of the S3-S4 linker in the *Shaker* potassium channel reveals two quenching groups near the outside of S4. *J. Gen. Physiol.* 115:209–222.

Starkus, J.G., L. Kuschel, M.D. Rayner, and S.H. Heinemann. 1997. Ion conduction through C-type inactivated *Shaker* channels. *J. Gen. Physiol.* 110:539–550.

Starkus, J.G., Z. Varga, R. Schonherr, and S.H. Heinemann. 2003. Mechanisms of the inhibition of *Shaker* potassium channels by protons. *Pflugers Arch.* 447:44–54.

Steidl, J.V., and A.J. Yool. 1999. Differential sensitivity of voltage-gated potassium channels Kv1.5 and Kv1.2 to acidic pH and molecular identification of pH sensor. *Mol. Pharmacol.* 55:812–820.

Trapani, J.G., and S.J. Korn. 2003. Effect of external pH on activation of the Kv1.5 potassium channel. *Biophys. J.* 84:195–204.

Wang, Z., J.C. Hesketh, and D. Fedida. 2000. A high-Na^+ conduction state during recovery from inactivation in the K^+ channel Kv1.5. *Biophys. J.* 79:2416–2433.

Yang, Y., Y. Yan, and F.J. Sigworth. 1997. How does the W434F mutation block current in *Shaker* potassium channels? *J. Gen. Physiol.* 109:779–789.

Zhang, S., C. Eduljee, D.C. Kwan, S.J. Kehl, and D. Fedida. 2005. Constitutive inactivation of the hKv1.5 mutant channel, H463G, in K^+-free solutions at physiological pH. *Cell Biochem. Biophys.* 43:221–230.

Zhang, S., H.T. Kurata, S.J. Kehl, and D. Fedida. 2003. Rapid induction of P/C-type inactivation is the mechanism for acid-induced K^+ current inhibition. *J. Gen. Physiol.* 121:215–225.